Colombian Volcanic Ash Soils

M.C. Herrera & A. Lizcano
Los Andes University, Bogotá, Colombia

J.C. Santamarina
Georgia Institute of Technology, Atlanta, USA

1. INTRODUCTION

Volcanic ash soils formed from the weathering of materials ejected during volcanic eruptions. They are found in regions with intense volcanic activity such as the Pacific Ring of Fire. Approximately 60% of the soils in tropical countries are volcanic ash soils (Quantin, 1986; Shoji et al., 1993).

Volcanic eruptions have occurred during the last 20,000 years in the Andes Range in Colombia (Pleistocene and Holocene – Quaternary period). The location of major volcanoes and the correlated distribution of volcanic ash soils are shown in Figure 1. In the central region, they coincide with the Coffee Zone and the departments of Antioquia, Caldas, Risaralda and Quindio. In the southwestern region, they are found in the departments of Tolima, Huila, Cauca, Valle del Cauca and Nariño. And in the eastern areas, volcanic ash soils are distributed in a random pattern (Bogota and Llanos Orientales). These deposits play an important role in agriculture, especially for upland crop production.

2. ENGINEERING GEOLOGY

2.1. *Source of material – "Volcanic Ash"*

Volcanic eruptions start with the ejection of pyroclasts. The cloud of pyroclasts is formed by volcanic ashes which are made of solidified magma or crust fragments that range in diameter from 0.2 μm up to 2mm. The primary mechanisms in volcanic ash formation include magma vesiculation (i.e. gases expand rapidly and generate voids called vesicles), magma fragmentation by very high thermal or mechanical stresses generated by the interaction with near-surface water, and comminution or pulverization of lava or crust materials from vent walls (Wohletz & Krinsley, 1982; Büttner et al., 1999).

The energy liberated during the eruption determines the size and elevation reached by the dust cloud. Volcanic ashes can raise several kilometers into the atmosphere and can be transported hundreds of kilometers away from the source by strong wind currents. Some ashes can remain suspended for days or months in the atmosphere. Particle shape (sphericity and roughness), size and specific surface, chemical composition and electrostatic charge determine travel distance away from the source and settling velocities (Riley et al, 2003).

Volcanic ash particles have an initial blocky or vesicular shape. Blocky particles have planar surfaces resulting from the brittle breaking of frozen lava. Vesicular ashes have drop-like shape. Friction and abrasion during transport tend to reduce roughness and increase sphericity.

The particle size distribution in deposited volcanic ash is correlated with traveled distance: coarser ashes are found at shorter distances. However, small particles (diameter < 20 μm) are often lightly attached to each other or to the surface of the larger particles through electrostatic forces and capillary forces generated by fluids within the cloud (such as sulphuric acid H_2SO_4). Such an aggregation contributes to the wide variation of grain size distribution commonly found in ash deposits, and the presence of fine particles near volcanoes (Gilbert et al., 1991).

The mineralogy of volcanic ashes determines the mass density and the development of electrical charge before deposition. Both light (G_s<2.8-3.0) and heavy (G_s>2.8-3.0) minerals are present in volcanic ashes; light minerals dominate and represent between 70% and 95% of the mineral content (Shoji et al., 1993). Most volcanic ashes contain (Nanzyo, 2004): volcanic glass (G_s=2.2-2.4), felspars (G_s=2.6-2.7), quartz (G_s=2.6-2.65), hornblend (G_s=3-3.4), hypersthene (G_s=3.2-3.9), augite (G_s=3.2-3.6), magnetite (G_s=4.5-5), biotite (G_s=2.9-3.4) and apatite (G_s=3.1-3.2). Volcanic glass predominates among of primary minerals; it has a poorly ordered structure and exhibits very low resistance to chemical weathering (Tazaki et al., 1992; Shoji et al., 1993).

Volcanic ashes can be classified by composition, with emphasis on total silica content. In descending order of total silica content, volcanic ashes are catalogued as: rhyolite, dacite, andesite, basaltic andesite and basaltic (Shoji et al., 1993). Colombian volcanic ash soils are derived from andesitic and dacitic ashes that were rich in plagioclase, volcanic glass, amphibole and pyroxene and poor in quartz (Arango, 1993).

2.2. *Post-depositional processes – "Volcanic ash soils"*

Volcanic ash soils are residual deposits that evolve in situ from volcanic ashes. The diagenetic processes include the dissolution of base minerals, the precipitation of new complexes such as clay minerals, and the development of a new structure, fabric and particle arrangement. A schematic representation of the formation of these soils is shown in Figure 2.

Time and climate (precipitation, temperature, humidity and air flow) determine the evolution of diagenetic processes. Old and highly weathered deposits are fine and clayey, while young and lightly weathered deposits are sandy and coarse. The original mineralogy of volcanic ashes affects the weathering rate. Acidic rocks such as quartz, feldspars, hornblende and micas are more resistant to weathering than basic rocks such as olivine, pyroxenes and calcium plagioclase (Townsend, 1985). Water availability controls dissolution and reprecipitation, the rate of chemical reactions, and the efficient leachage of soluble components (Townsend, 1984; Chadwick et al., 2003).

As weathering progresses, Si, Ca and Na are leached away, and the Al left behind prevails in the composition of new minerals (Nanzyo, 2004). In arid areas, soluble weathering products such as Si and base cations are leached from superficial areas and less soluble components such as Al do not move. In humid regions, all main elements are leached from the top of the layer; base cations, Si and Al reduce in amounts that depend on the parent material (Ziegler et al, 2003). In such humid environments, the formation of gibbsite and aluminosilicate clays is minimized when there are high levels of organic matter that can preferentially absorb aluminum (Shoji et al., 1993). The recharge of cations on the exchange complexes increases as rainfall and leaching intensity increase. Leaching determines the rate of loss of cations and hence the rate of acidification. Even though leaching depends on rainfall, it is more directly dependent on the effective moisture, which is the relation between water holding into pores and leaching intensity (Chadwick et al., 2003).

While leaching has controlled the formation of Colombian volcanic ash soil deposits, erosion affects its accumulation. Therefore, the most abundant and thickest volcanic ash soil deposits are found in cold regions while deposits of moderate thickness are found in warm and wet environments (Arango, 1993). Moreover, slightly undulating and planar topographies have contributed to the formation of thick deposits, while steep areas are characterized by thin deposits due to erosion and stripping. The thickness of volcanic ash soil deposits in the Coffee Zone varies from less than 1 m on 45° slopes to 10-to-20 m in flat areas (Terlien, 1997).

Colombian volcanic ash soils exhibit high spatial variability in their physical properties, such as color, consistency, moisture, mineralogy, and dry density. Coarser grained deposits are found closer to Pereira, while finer grained deposits are closer to Armenia due to their relative distance to active volcanoes (see Figure 1). Higher sand content is commonly present in shallower layers (young deposits) and higher clay contents are found in deeper older layers. High pyroxene content is correlated with sandy textures, while the abundance of amphibole leads to silty and clayey textures (Arango, 1993). A general soil profile is shown in Figure 3.

2.3. *Stress history*

These deposits have not been pre-stressed by overburden. However, seasonal wetting-drying cycles and associated capillary effects are pronounced in the Coffee Zone. The water table is usually found deeper than 10 m, within the fluvio-volcanic layer. Seasonal changes in water elevation ranges between 2 m and 4 m. A reddish thin seam of iron oxide is often found as an indicator of a prehistoric water table. A perched water table above the contact between the layer of volcanic ash soil and the underlying fluvio-volcanic layer can be found during rainy periods as a result of the marked difference in hydraulic conductivity between the two layers.

The mechanical properties of Colombian volcanic ash soils are determined by their structural formation features rather than by their stress history. In particular, their inherent cementation governs their mechanical behavior, as discussed in subsequent sections.

3. PHYSICO-CHEMICAL PROPERTIES

The mineralogical composition of volcanic ash soils is characterized by the presence of clay minerals that are uncommon in sedimentary soils. These minerals include: allophane, imogolite, halloysite, ferrihydrite or Al/Fe-humus complexes, and opaline silica. Al/Fe-humus complexes and opaline silica form in acidic environments ($pH \leq 5$) which are rich in organic matter. Allophane, imogolite, halloysite, and ferrihydrite form in environments with $5 \leq pH \leq 7$ and low organic matter content (Ugolini & Dahlgren, 2004).

Volcanic glass is one of the main primary components in volcanic ash. It is thermodynamically unstable and weathers readily. During a typical weathering sequence, volcanic glass transforms into allophane, halloysite, methahalloysite, kaolinite and montmorillonite (Fisher & Schmincke, 1984; Murray et al., 1977). This sequence suggests the predominance of allophane in young volcanic ash soils and of halloysite in older deposits - for the same parent material and weathering conditions.

The mineralogical analysis of Colombian volcanic ash soils shows the predominance of volcanic glass, feldspar plagioclase and quartz in the coarser silt and sand fractions (Table 1). The clay fraction contains hydrated halloysite (> 50%), moderate amounts of cristobalite, some traces of feldspars and material non quantifiable by XRD (Figure 4). It is anticipated that allophane is present in the percentage of clay material non quantifiable by XRD since the sodium fluoride test used to identify the presence of allophane returned a positive result (procedure as in Fieldes & Perrott, 1966): the indicator paper treated with phenolphthalein turned red when a small amount of soil was added indicating that pH exceeds 9 as the sodium fluoride caused the release of hydroxyl ions from the allophane in amounts much larger than from other clay minerals.

Grain size distribution analyses (sieve and hydrometer) show the predominance of silt and clay size particles (see Table 2 and Figure 5). However these results need careful interpretation since particle size distribution results are strongly affected by specimen preparation in these soils. Drying produces irreversible changes in structure and the extent of grinding determines the size of surviving aggregations. Additionally, clay minerals such as allophone have a strong flocculating tendency at $pH \approx 6$, and sodium hexametaphospate is only partially effective in dispersing volcanic ash soils (Wesley, 1973; Maeda et al., 1977, Rouse et al, 1986; Shoji et al., 1993; Rao, 1995). Data in Figure 5 are gathered using sodium hexametaphospate (ASTM D422-63 1998) and confirmed with tests run with different concentrations of a commercially available dispersant (Colloid 260 made by Rhône-Poulenc).

The specific surface and pore size distribution of Colombian volcanic ash soils are investigated using N_2 gas adsorption and desorption experiments (Nova 1200 Quantachrome). Specimens are placed into a cell and outgassed at 100°C for a period of 4 h. During measurements, the temperature is maintained constant in a liquid-N_2 bath. The measured specific surface ranges between $S_s=147\ m^2g^{-1}$ and $S_s=177\ m^2g^{-1}$ (BET method). Additionally, the methylene blue adsorption method was used to obtain the surface available under wet conditions. The specific surface values vary between S_s=245 m^2g^{-1} and S_s=360 m^2g^{-1}. Both wet and dry results evidence the presence of very fine clay particles, in agreement with the detected halloysite and allophane components.

The equivalent particle dimension calculated from specific surface values varies between 6 and 9 nm for spherical particles (diameter=$6/(S_s\rho G_s)$), 4 nm and 6 nm for prismatic particles (length>>width, width=$4/(S_s\rho G_s)$) and, 2 and 3 nm for thin platy particles (thickness=$2/(S_s\rho G_s)$).

The pore size distribution is evaluated by applying BJH method to the N_2 gas desorption isotherm data. Results show a peak for pore diameters ~25 nm and ~170 nm (Figure 6).

Scanning electron microscopy SEM provides further insight into structural features and the distribution of particles and pores in undisturbed specimens. SEM images in Figure 7 show clusters of particles with an equivalent diameter ranging between 2.5 μm and 75 μm. Individual particles become visible at submicron resolution and consist of randomly oriented halloysite cylinders derived from volcanic glass weathering; they connect their extremes in a finger-like pattern. The length of individual cylinders varies between 0.46 and 0.66 μm and their mean diameter is 0.1μm.

The large pores observed in SEM images (Figure 7a) have an equivalent diameter ranging from 4.5 μm to 10 μm. Pores between clusters have an equivalent diameter of ~0.5 μm to ~2 μm. At the particle level, pores are controlled by the arrangement of individual particles and are smaller than 500 nm.

The in situ pH is 6.5, in agreement with allophane, imogolite (pH=5 – 7, Wada, 1989) and halloysite formation (pH=5.7 – 7.1, Wada, 1990). The cation exchange capacity CEC is determined by Na exchange at the in situ pH. The CEC increases as the clay content increases with depth: CEC=11.9 cmol(+)/kg for the z=5.5 m specimen, and CEC=38.7 cmol(+)/kg for the z=7.0 m specimen. These results are similar to those reported for volcanic ash soils in Costa Rica (CEC=20 – 50 cmol(+)/kg – Wada, 1989) and Honduras (CEC=50.0 cmol(+)/kg – Fassbender, 1987). Halloysite, the most abundant clay mineral in these soils, is responsible for the measured cation exchange capacity.

The water retention properties reflect the interaction between the mineral, the fabric and water. The filter paper, salt solutions and porous plate techniques are used to determine the water retention curves of Colombian volcanic ash soil specimens. Results are presented in Figure 8 for specimens gathered at two depths. The pronounced differences between these results confirm the high variability in soil properties with depth.

The characteristic curve for the shallower, coarser and denser specimen (z=5.5 m) is in a narrow range of water content (w_o= 10%-to-43%). The characteristic curve for the deeper, finer and more porous specimen (z=7.0 m) covers a wide range of water content (w_o= 46%-to-110%). Both specimens exhibit moderate changes in suction when the moisture $w>w_P$. The high water retention capacity in these soils is associated to the high specific surface, pore structure and pore size distribution, and the presence of allophane minerals that may retain water inside the hollow spherules (Lu & Likos, 2004; Ranst et al., 2002).

4. STATE AND INDEX PROPERTIES

Volcanic ash soils are characterized by very high void ratio, water retention and high plasticity. Reported index properties of volcanic ash soils around the world and in Colombia are summarized in Table 2, including values gathered as part of this study.

Drying and remolding alter the properties and behavior of volcanic ash soils and render the traditional soil classification methods inadequate (Knight, 1986). In the undisturbed state, volcanic ash soils appear as a low water content silty sand with little or no plasticity. However, they lose particle bonding when remolded, their moisture becomes apparent and they exhibit a highly plastic behavior (see also NZ Geotechnical Society, 2003).

Drying alters plasticity and water retention. The high plasticity in the natural condition decreases after either air or oven drying as is shown in Table 3. The loss in plasticity depends on the initial water content, drying temperature, and the duration of desiccation (Warkentin &

Maeda, 1974; Maeda et al., 1977; Wada & Wada, 1977; Lohnes & Demirel, 1983; Wells & Northey, 1984; Townsend, 1985; Moore & Styles, 1988; Wells & Theng, 1988; Wesley, 1996; Pandian et al., 1993; Shoji et al., 1993; Wan et al., 2002; Wesley, 2003). The extent of irreversible plasticity loss remains unclear.

Plasticity data for Colombian volcanic ash soils are plotted in Figure 9. The data fall below the A-line. While halloysite renders low liquid limit and plasticity, the presence of allophane increases the Atterberg limits of these soils (Rao, 1996).

5. ENGINEERING PROPERTIES

5.1. *Zero lateral strain k_o loading (Constrained modulus)*

The constrained modulus of Colombian volcanic ash soils is measured in oedometer tests carried on undisturbed and remolded specimens made of material extracted as block specimens (Coffee Zone – Manizales). Undisturbed specimens are carefully hand-trimmed to minimize disturbance. Remolded specimens are formed with oven-dry, crushed material. Tests are repeated with different size fractions to explore the effects of the degree of remolding. Undisturbed specimens are tested at their natural water content and under saturation condition.

Undisturbed specimens are saturated before loading by submerging them in water while monitoring changes in specimen height; no volumetric changes are registered as capillary forces vanish. Remolded specimens are saturated at σ_v'=72 kPa which corresponds to the in situ vertical stress.

Characteristic results are presented in Figure 10. The e–σ_v' trend for the undisturbed specimens starts at a high void ratio (e= 3.7). The yield stress is reached at σ_v'= 200–to–300 kPa; following from previous discussions, it is anticipated that this yield stress is not due to pre-loading but to the physical-chemical formation history (see also Wesley, 1973 and 2001).

The low stress $\sigma_v'<\sigma_y'$ compressibility is low (C_c= 0.19–to–0.29) as inherent cementation inhibits compression (there is not suction in saturated specimens). The application of a high vertical stress $\sigma_v'>\sigma_y'$ damages interparticle bonds, and the sediments gain the high compressibility (C_c= 1.11–to–1.22) expected for high void ratio clayey soils. Unloading and reloading follow similar paths and the recompression coefficient varies between C_r= 0.08 and C_r= 0.12.

Remolded soil specimens are prepared to attain the highest possible void ratio in order to resemble the open structure in undisturbed specimens. However, it is not possible to repack soil grains at a void ratio higher than e=2.2-to-2.7 (Figure 10). The e–σ_v' behavior is stress controlled in all the stress range and remolded specimens exhibit high compressibility (C_c= 0.35–to–0.61).

The role of stiffness on the time-rate of consolidation is highlighted in Figure 11 where the value of C_v for each loading stage is plotted versus σ_v' (undisturbed specimens). At low stress $\sigma_v'<\sigma_y'$, consolidation occurs fast and the C_v coefficient varies slightly with stress; its value C_v=2.0-to-2.4 cm^2s^{-1} is similar to silts. Beyond the yield stress $\sigma_v'>\sigma_y'$, the cemented soil skeleton deteriorates and the consolidation rate becomes markedly slower approaching values similar to clays (C_v=0.022-to-0.056 cm^2s^{-1}).

5.2. *Small-strain stiffness – Shear wave velocity*

The oedometer tests reported above are performed in a cell instrumented with bender elements to study the evolution of stiffness in both undisturbed and remolded specimens during loading, unloading and reloading. Characteristic results are summarized in Figure 12.

Saturated undisturbed specimens show very low V_s sensitivity to effective stress at low stress, $\sigma_v'<\sigma_y'$. Assuming a power equation $V_S = \alpha\left(\sigma_v' / kPa\right)^{\beta}$, the β-exponent is very low (β=0.059), in agreement with particle cementation (in the absence of suction). When the vertical stress exceeds the yield stress $\sigma_v'>\sigma_y'$, the β-exponent increases to β=0.28. This denotes the sudden structural decementation and decisive volume change with increased stresses. For comparison, the remolded specimens exhibit high β-exponent (β=0.50) within the applied range of vertical stress.

In spite of the cementation in undisturbed volcanic ash soil specimens (high void ratio), their shear wave velocity is lower than the shear wave velocity of remolded specimens (lower void ratio) in the typical stress relevant for engineering applications ($\sigma_v' > 100$ kPa). It is important to note that cemented sands and silts have higher shear wave velocity than their uncemented counterparts at all stress levels. This unique characteristic of volcanic ash soils remarks their exceptional formation history.

5.3. *Shear strength*

The shear strength of Colombian volcanic ash soils depends on the degree of diagenesis. The drained shear strength of saturated undisturbed specimens is studied using direct shear and undrained triaxial compression tests. These silty specimens (location: Manizales; depth: 5.5 m) have a void ratio e=1.34, and a high amount of primary minerals such as volcanic glass and plagioclase feldspar which denote a young soil.

Direct shear test results are shown in Figure 13. The peak shear strength shows a friction angle φ=32°–34°. For comparison, published friction angle and undrained strength data are summarized in Table 4.

Consolidated undrained triaxial test data gathered for saturated undisturbed specimens are shown in Figure 14 (location: Manizales; depth: 5.5 m). The first yield is observed at $\varepsilon_1 \approx 0.2\%$. The brittle strain-stress response reaches the peak at an axial strain of $\varepsilon_1 \approx 2\%$. The critical state line has a slope of M=1.2 which corresponds to an axial-compression friction angle of φ=30°.

5.4. *In situ testing: penetration resistance*

In situ SPT data provide further information into the peculiar properties of Colombian volcanic ash soils. In general, SPT values are lower than N=10, and they usually range between N=4 and N=8. The interpretation of SPT results needs careful consideration for volcanic ash soils: the SPT induces a high strain level that is not representative of common engineering conditions and fails to sense the low compressibility of volcanic ash soils. Maeda et al. (1977) proposed the following correlation between the N-value of allophanic soils and the bearing capacity $q_a=(2 \text{ to } 2.5)N$. The coefficient is higher than that found for non-volcanic soils at the same water content (i.e. 1 to 1.3).

5.5. *Hydraulic conductivity*

A wide range of hydraulic conductivity values has been reported for Colombian volcanic ash soils (Table 4). In general, volcanic ash soils tend to be more permeable than it is expected for soils with such a high specific surface (Wesley, 1977). This is related to the intercluster porosity (Figure 7).

The hydraulic conductivity values inferred from consolidation data range between $k=7\text{x}10^{-8}$–to–$13\text{x}10^{-8}$ m/s for undisturbed specimens at low stress $\sigma_v' < \sigma_y'$. The hydraulic conductivity appears stress-dependent beyond the yield stress, and it decreases markedly, reaching $k=1.9\text{x}10^{-9}$ m/s at $\sigma_v' = 636$ kPa.

It has been observed that environmental changes modify conduction properties in volcanic ash soils. In particular allophonic soils develop positive surface charge at low pH and tend to swell; this causes a decrease in large pores and a reduction in hydraulic conductivity (Ishiguro & Nakajima, 2000). Wet-dry cycles can have an important effect on hydraulic conductivity of shallow layers through the formation of fracture networks.

5.6. *Electrical conductivity*

The electrical conductivity of the pore fluid determines the electrical conductivity of the sediment, yet reduced by the porosity and the degree of saturation (Archie´s law). Ionic concentration and valence define the pore fluid conductivity. The double layer around minerals adds surface conduction: the higher the specific surface of the soil the higher the contribution of surface conduction.

The electrical conductivity σ_E of the pore fluid in Colombian volcanic ash soils varies between σ_E=0.21 dS/m and σ_E=0.23 dS/m for specimens at z=5.5 m and z=7.0 m, respectively (Location: Manizales). These values indicate low ionic concentration which may be a consequence of good drainage conditions. The equivalent osmotic pressure derived from electrical conductivity values is π=7.6 kPa and π=8.4 kPa (according to McBride, 1994) and π=6.0 kPa y π=6.6 kPa (according to USDA, 1950).

The high resolution electrical profile shown in Figure 15 is measured from the top towards the bottom of the specimen (height=4 cm) using an electrical needle probe (diameter: 2.18 mm, Lee et al. 2005). The uniform profile suggests high homogeneity at the meso-scale.

5.7. *Thermal conductivity*

The thermal conductivity of dry soils is related to porosity, contact quality, and degree of saturation. The thermal conductivity k_t of undisturbed Colombian volcanic ash soils is measured using the thermal needle probe technique (Yun & Santamarina, 2005). Results show an average value of k_t =0.71 W/mK for a water content w_o=115%. The volume fraction of air for this specimen is $V_a/V_{tot}\approx 0.13$, and the trend by Tang et al. (2005) predicts k_t~0.85. Results reported for other volcanic ash soils include: Japanese allophanic soils k_t =0.5 – 0.7 W/mK, Japanese andisols k_t =0.6 – 0.8 W/mK (Maeda et al., 1977), and Chilean andisols k_t =0.84 – 0.94 W/mK (water content ranging between w_o=30% and w_o=33% – Antilen et al., 2003).

6. ENGINEERING PROBLEMS

6.1. *Degradation due to drying and wetting cycles*

Dessication effects depend on climatic conditions (evaporation rate, temperature gradients, precipitation, etc.), water table and vegetation (Naser & Drobroslav, 1995). Colombian soils in the Coffee Zone are subjected to frequent drying and wetting cycles. Typically, a long rainy period occurs during April-May, and a second one in October-November. Each of these wet periods is followed by a severe dry period.

These sequential dry-wet periods lead to dessication crack formation as it is readily observed in all exposed cuts (Figure 16). The desiccation of a saturated soil and the development of desiccation fractures progresses in stages:

- First, water evaporation increases suction and the soil contracts while the surface remains saturated (Aitchinson & Colmes, 1953). During this stage, the volume change equals the moisture loss, and it is determined by the clay content, mineralogy, texture and structure (Aitchinson & Holmes, 1953; Baer & Anderson, 1997).
- As the soil gets denser, the resistance to contraction increases and air finally enters into the soil structure, and desiccation propagates into the soil volume at almost constant volume; this is the upper limit of residual contraction (Aitchinson & Holmes 1953; Bronswijk, 1991; Colina & Roux, 2000). Particle aggregation due to drying transforms microspores into macrospores and results in a reduction of the water-holding retention capacity.
- During the last stage of the desiccation, the soil volume remains constant and water loss equals air volume entering into the soil. The transition between the residual contraction and the null contraction stages is defined as the lower limit of residual contraction (Bronswijk, 1991; Colina & Roux, 2000).
- The spatial variability of moisture content produces differential suction stresses and local contraction leading to crack formation. Cracks grow in length as well as in depth until the contraction is insufficient to cause further crack propagation.
- New cracks propagate towards preexistent cracks intersecting them at ~90°. Secondary cracks are usually initiated at the middle of the longest side of a preexistent block where contraction is highest (Morris et al., 1992; Jagla, 2004).

Therefore, dessication cracks form a pattern of polygonal blocks (with 4 – 6 sides) with a size that is proportional to the width of the drying layer (Colina & Roux, 2000; Jagla, 2004).

Large cracks are more prone to form than shorter ones because larger cracks need lower contraction to propagate. The contraction across a crack is inversely proportional to the square of the crack length $[L]^{-0.5}$. Moreover stresses redistribute in the presence of adjacent cracks (Morris et al., 1992).

Dry conditions cause irreversible aggregation and crack formation on slopes in volcanic ash soils. In fact, altitude and slope orientation towards the sun are the main factors influencing the deterioration of slopes in the Colombian Coffee Zone (Imeson & Vis, 1982).

Drying (11 hrs) and wetting (1 hr) cycles are imposed Colombian volcanic ash soil specimens to corroborate the effect of dessication cycles on slope deterioration. Specimens are 50 mm large cubes trimmed from undisturbed block samples. Results are summarized in Figure 17. The data in Figure 17-a show the controlling effect of temperature on water loss. The data in Figure 17-b show the effect of temperature and cycles: no cracks are observed after 9 cycles when drying cycles take place at T=20°C, 30°C or 40°C. However specimens show large fractures after the second drying cycle when T=45°C, and after just the first drying cycle when T=50°C.

6.2. *Compaction and collapse upon saturation*

Figure 18 shows the compaction curve for a relatively young and dense specimen (e_o=1.3 – location: Manizales, depth: 5.5 m). Older, finer and more porous volcanic ash soils tend to exhibit even more elusive peaks. In fact, an old volcanic ash soils that have not experienced severe desiccation may not display a distinct maximum dry density or an identifiable optimal water content. However, even in this case, the compaction response becomes more conventional after drying and rewetting. Apparently, suction induced aggregation renders a less plastic material made of silt-size clusters. The natural moisture content in the field is typically wetter than the optimum water content obtained in the laboratory with previously dry material. Therefore construction procedures require drying before compaction.

Distinct construction techniques have been developed for these soils to control the compaction effort and the extent of drying. The compaction energy has an important effect: as the number of blows increases or heavy machinery is used in field, soil strength reduces markedly during compaction as the soil structure is progressively destroyed and water is released (Wesley, 2003).

These observations suggest that conventional compaction specifications are not applicable to these materials. Dr. Millan (Personal Communication – Pereira) has successfully demonstrated through numerous case histories an alternative approach that consists of excavating the borrow material and placing it with minimal disturbance. Low energy, light compaction equipment is used to attain a density similar to the original one in situ and at the same natural water content.

This methodology is experimentally evaluated using oedometric tests. Figure 19 shows the e–σ_v' response of the specimen compacted to the in situ density and water content. The structural stability of an identical specimen is evaluated by enforcing saturation at σ_v' =100 kPa. The load-deformation response is very similar for both specimens and there is only a small volume reduction upon saturation at σ_v' =100 kPa (collapse index $I_c=\Delta e/(1+e_o)$=0.33%).

Additional tests are run to determine the collapse potential of intact soil (ASTM: D5333, 1996). Several undisturbed, unsaturated specimens are loaded to preselected values of vertical effective stress (σ_v'=100-to-1600 kPa). Then, specimens are saturated. Results in Figure 20 show contraction in all cases, with a small collapse index I_c <1%. This low collapse potential confirms the presence of insoluble cement bonding.

6.3. *Slope stability*

Cementation and suction are important contributors to slope stability in volcanic ash soils. Natural slopes in these deposits tend to be much steeper than those in sedimentary soils. In fact, natural and man-made slopes in Colombian volcanic ash soils may exceed 20 m with slopes angles higher than 60° (Forero et al., 1999; Redondo, 2003) even thought, friction angles are lower than $\varphi\sim34°$. However these slopes and cuts are susceptible to gradual instability and surface degradation depending on the climatic conditions and vegetation cover. The orientation of the slope with respect to the sun has a decisive effect.

Frequent landslides in the Coffee Zone have produced many deaths and economic losses. The most common trigger mechanisms are: heavy rainfalls and earthquakes, aggravated by loss of forest cover, non-planned land use, and poor waste water management. The annual precipitation in the Coffee Zone ranges between 1500 mm and 2250 mm. Rainfalls higher than 70 mm in one or two days (Terlien, 1997; Cuadros & Sisa, 2003) triggers shallow landslides with depth<1.5 m. Deeper landslides are triggered by precipitation higher than 200 mm during 25 days followed by a low daily rainfall (< 50 mm – Terlien, 1997). Slope failures also occur after a heavy rainfall during a very dry period (January-February and July-August).

Shallow slope failures in Colombian volcanic ash soils develop a planar, translational slide. Deeper failures (3-to-10 m) present more irregular slide surfaces. The sliding surface is commonly formed along the contact between the volcanic ash layer and the underlying fluvio-volcanic deposit (Forero et al., 1999; Cuadros & Sisa, 2003). Dramatic permeability differences between these layers lead to an increase pore pressure in perched water tables (Ng et al., 2003). In addition, the network of dessication fissures fills during rainfalls and prompts failures.

High magnitude earthquakes have high recurrence in the Coffee Zone. Manizales is 15 km away from seismotectonic zone capable of generating earthquakes at depths ranging between 10 km and 13 km and Richter magnitudes greater than 6 (Valencia, 1988). In this region, earthquakes have triggered slides in steep slopes in both residual and colluvial materials (Terlien, 1997). The distance from the epicenter, frequency and event duration determine the earthquake effect on slope stability. Rodriguez (2002) shows that slope failures in volcanic ash soil deposits are triggered when the seismic peak velocity of 0.09 m/s for earthquakes originate in the Subduction Zone, or when the seismic peak velocity exceeds 0.23 m /s for earthquakes that originate in the Earth´s crust (Redondo, 2003).

7. CONCLUSIONS

- The evaluation of volcanic ash soils for engineering applications demands a rigorous understanding of their structure, mineralogy, and formation history.
- Volcanic ash soils result from the in-situ diagenesis of volcanic ashes. The main processes involved are the dissolution of original minerals, selective leachage, and re-precipitation of new minerals.
- Diagenesis produces changes in particle size (from silt and sand size to clay-size), increase in void ratio (from $e<1$ in volcanic ash, to $e>2$ in volcanic ash soils), and changes in mineralogy (from initial volcanic ash minerals, to allophane, imogolite and halloysite).
- Volcanic ash soils have a cemented, highly porous granular structure, with low stress dependent stiffness and low compressibility below the yield stress. Inter-particle aggregation imparts a misleading silt-like soil appearance.
- The unique formation history affects all forms of conduction, including hydraulic, thermal and electrical.
- Stress-strain behavior varies considerably when soils are disturbed (i.e. overloading, drying, etc.). Geotechnical problems and construction techniques associated with these materials are directly linked to the magnitude of the disturbance produced.
- Traditional classification methods are inadequate for volcanic ash soils. Drying and remolding practices modify plasticity, stiffness, strength. Likewise, data from in situ tests require careful interpretation.
- The water retention potential of volcanic ash soils reflects the formation history. Mature volcanic ash soils have inter-aggregate and intra-aggregates porosity and high clay content, and develop high suction.
- High and steep natural and man-made slopes in the field manifest the contribution of both cementation and suction to soil strength.
- Drying and wetting cycles cause dessication cracking and soil deterioration. The effects depend on temperature and the duration of the drying period. Dessication cracking is the prevailing mechanism in the degradation of slopes and cuts.

- Compaction causes desegregation, the release of water in pores, and the manifestation of the soil as a high specific surface clayey sediment. Alternative compaction techniques have been suggested for volcanic ash soils, including minimal compaction to preserve the in situ soil structure.

REFERENCES

Aitchinson, G.D. & Holmes, J.W. 1953. Aspects of swelling in the soil profile. *Aust.J.Appl.Sci*. 4: 244-259

Antilen, M. Escudey, M, Forster, J.E., Moraga, N. Marty, D. and Fudym, O. 2003. Application of the hot sick method to the thermophysical characterization of soils. *Journal of the Chilean Chemical Society* 48(3).

Arango, J.D. 1993. Características generales y comportamiento geotécnico de las cenizas volcánicas en la Zona del Antiguo Caldas. Unpublished Msc. Theses. Universidad de Los Andes. Bogotá.

Baer, J.U. & Anderson, S.H. 1997. Landscape effects on desiccation cracking in an Aqualf. Soil Sci. Soc. Am. J. 61:1497-1502.

Benavides, G. 1982. El intercambio aniónico como criterio de diferenciación de suelos derivados de cenizas volcánicas. Colombia Geográfica, Vol. 9, No.2, pp. 99-109.

Bronswijk, J.J.B. 1991. Relation between vertical soil movements and water-content changes in cracking cáliz. *Soil Science Society of American Journal* 55: 1220-1226.

Büttner, R., Dellino, P. & Zinranowski, B. 1999. Identifying magma – water interaction from the surface features of ash particles. *Nature* 349: 668.

Chadwick, O.A. Gavenda, R.T. Kelly E.F. Ziegler, K. Olson, C.G. Elliott, W.C. & Hendricks, D.M. 2003. The impact of climate on the biogeochemical functioning of volcanic soils. *Chemical Geology* 202: 195-223.

Colina, H. & Roux, S. 2000. Experimental model of cracking induced by drying shrinkage. *The European Physical Journal E* 1:189-194.

Cuadros, O. & Sisa, R. 2003. Relación lluvia-deslizamientos en Manizales y sus alrededores. Colombia National University. Civil Engineering Department.

Deka, R.N. Wairiu, M. Mtakwa, P.W. Mullins, C.E. Veenendaal, E.M. and Townsend, J. 1995. Use and accuracy of the filter-paper technique for measurement of soil matric potential. *Eur. J. Soil Sci*. 46: 233-238.

Fassbender, H.W. 1987. *Química de suelos con énfasis en suelos de América Latina*. Servicio Editorial IICA. San José, Costa Rica.

Fawcett, R.G. and Collis-George. 1967. A filter-paper method for determining the moisture characteristics of soil. *Aust. J. Exp. Agr. Anim. Husb*. 7 : 162-167

Fieldes, M & Perrot, K.W. 1966. The nature of allophane in soils. *New Zealand Journal of Science* 9:623-629.

Fisher, R.V. & Schmincke, H.U. 1984. *Pyroclastic Rocks*. Spronger-Verlag, Berlin.

Forero-Dueñas, C. Gálvez, P. Fino, & Ulloa. 1999. Estudios de la estructura de las cenizas volcánicas de Armenia y su relación con el comportamiento geotécnico. *X Jornadas Geotécnicas de la Ingeniería Colombiana* Boletín Colombiano de Geotecnia. Sociedad Colombiana de Geotecnia.

Gilbert, J.S. Lane, S.J., Sparks, R.S.J. & Koyaguchi, T. 1991. Charge measurements on particle fallout from a volcanic plume. *Nature* 349: 598.

IGAC. 1995. *Suelos de Colombia: origen, evolución, clasificación, distribución y uso.* Instituto Geográfico Agustín Codazzi. Bogotá, Colombia.

IGAC. 1996. *Suelos: Departamento del Quindio*. Instituto Geográfico Agustín Codazzi - Subdirección Agrológica. Bogota, Colombia.

Imeson, A.C. & Vis, M. 1982. A survey of soil erosion processes in tropical forest ecosystems on volcanic ash soils in the Central Andean Cordillera, Colombia. *Geografiska Annaler. Series A, Physical Geography*. 64(3/4).

Ishiguro, M. & Nakajima, T. 2000. Hydraulic Conductivity of an Allophanic Andisol Leached with Dilute Acid Solutions. *Soil Science Society of America Journal* 64(3):813-818.

Jagla, E.A. 2004. Maturation of crack patterns. *Physical Review E* 69, 056212.

Johnson – Maynard, J.L. McDaniel, P.A. Ferguson, D.E. & Falen, A.L. 1997. Chemical and mineralogical conversion of Andisols following invasion by Bracken Fern. *Soil Sci. Soc. Am. J*. 61:549-555.

Kitazono, Y. Suzuki, A. Kajiwara, M. & Aramaki, S. 1987. Contribution of micro structure to repeated loading effect on compacted allophaneous volcanic ash soil. *Soils and Foundations* 27(4): 23-33.

Knight, D.J. 1986. Geotechnical properties and behavior of the Monasavu halloysite clay, Fiji. *Clay Minerals* 21:311-332.

Lee, J. S., Fernandez, A. L., & Santamarina, J. C. 2005. S-wave velocity tomography: Small-scale laboratory application. *Geotechnical Testing Journal, ASTM* (Accepted).

Lohnes, R.A. & Demirel, T. 1983. Geotechnical properties of residual tropical soils In: *Geological Environment and Soil Properties*. Raymond N. Yong, (Ed.), Special Publication on Geological Environment and Soil Properties, ASCE Geotechnical. Engineering Division.

Lu, N. & Likos, W.J. 2004. *Unsaturated Soil Mechanics*. John Wiley & Sons, Inc.

Maeda, T. Takenaka, H. & Warkentin, B.P. 1977. Physical properties of allophane soils. In: *Advances in Agronomy*. N.C. Brady (Editor). Academic Press, Ney York, pp. 229-264.

McBride, M.B. 1994. *Environmental Chemistry of Soils*. Oxford University Press.

Mendoza, M.J. 1985 Remoldeling and drying effects upon plasticity limits of residual soils. *First International Conference on Geomechanics in Tropical Lateritic and Saprolitic Soils*. Brasilia, Brazil, Technical Sessions, 2:145 – 155.

Miura, S. 2003. Mechanical behaviour and particle crushing of volcanic course-grained soils in Japan. In: *Characterization and Engineering Properties of Natural Soils*. Tan et al. (Editors). P.p. 1169-1203.

Moore, P.J. & Styles, J.R. 1988. Some characteristics of a volcanic ash soil. *Geomechanics in Tropical Soils*. Proocedings of the Second International Conference in Tropical Soils. Singapore, 161.

Moroto, N. 1991. Mechanical behaviour of two typical compacted volcanic soils in Hachinohe, Japan under different sample preparation methods. *Soils and Foundations* 31(2):108-116.

Morris, P.H. Graham, J. & Williams, D.J. 1992. Craking in drying soils. *Canadian Geotechnical Journal* 29: 263-277.

Murray, H.H. Harvey, C. & Smith, J.M. 1977. Mineralogy and geology of Maungaparerua halloysite deposit in New Zealand. *Clays and Clay Minerals* 25 (1): 1-8.

Nanzyo, M. 2004. Unique properties of volcanic ash soils, *Global Environmental Research* Vol.6 No.2. Association of International Research Initiatives for Environmental Studies (AIRIES), Japan.

Naser, A. & Drobroslav, Z. 1995. Desiccation theory for soft cohesive soils. *Journal of Geotechnical Engineering* 121(6): 493-502.

New Zealand Geotechnical Society. 2003. Field description of soils and rocks. *Draft for comment. In: http://www.nzgeotechsoc.org.nz*

Ng, C.W.W. Zhan, L.T. Bao, C.G. Fredlund, D.G. & Gong, B.W. 2003. Performance of an unsaturated expansive soil slope subjected to artificial rainfall infiltration. *Géotechnique* 53(2):143-157.

O´Rourke, T.D. & Crespo, E. 1988. Geotechnical properties of cemented volcanic soils. *Journal of Geotechnical and Geoenvironmental Engineering* 114(10).

Olarte J.J. 1984. Suelos residuales en Colombia y su utilización en construcción de presas : primera etapa. *Publicaciones Uniandes*. Universidad de Los Andes. Bogotá, Colombia.

Olivares, L. & Picarelli, L. 2003. Shadow flowslides triggered by intense rainfalls on natural slopes coverd by loose unsaturated pyroclastic soils. *Géotechnique* 53: 283-287.

Pandian, N.S., Nagaraj, T.S. & Sivakumar Babu, G.I. 1993. Tropical Clays, II: Engineering Behavior. *Journal of Geotechnical Engineering* 119(5).

Parfitt, R.L. & Kimble, J.M. 1989. Conditions for formation of allophane soils. Soil *Sci. Soc. Am. J.* 53:971-977.

Quantin, P. 1986. Properties and genesis of Andisols. *Pédologue ORSTOM*, 70-74, Vol. XXII, No. 1, 105-111.Shoji S., Nanzyo M. and Dahlgren R.A. (1993) Volcanic Ash Soils: genesis, properties and utilization. Elsevier.

Rao, Sudhakar M. 1995. Mechanistic approach to the shear strength behavior of allophonic soils. *Engineering Geology* 40: 215-221.

Rao, Sudhakar M. 1996. Role of apparent cohesion in the stability of Dominican allophane soil slopes. *Engineering Geology* 43: 265-279.

Redondo, G.A. 2003. Comportamiento geomecánico de los materiales volcánicos aplicado a la estabilidad de taludes del Eje Cafetero. Unpublished Msc. Thesis. Civil Engineering Department. Colombia National University. Bogota, Colombia.

Riley, Colleen M. Rose, William I. Bluth & Gregg J. S. 2003. Quantitative shape measurements of distal volcanic ash. *Journal of Geophysical Research* 108(B10).

Rivera, J.D. 2003. Caracterización de las cenizas volcánicas en el departamento del Quindío sometidas a condiciones de secado. Unpublished Thesis in Civil Engineering. Los Andes University. Bogotá.

Rodríguez, P. 2002. Elements for Landslide Hazard Analysis in El Salvador. Civil Engineering Department. Colombia National University. Bogota, Colombia.

Rouse, W. 1986. Volcanic soil properties in Dominica, West Indies. *Engineering Geology* 23: 1-28.

Sahaphol, T. & Miura, S. 2005. Shear moduli of volcanic soils. *Soil Dynamics and Earthquake Engineering* 25:157-165.

Shoji, S. Nanzyo, M. & Dahlgren, R.A. 1993. *Volcanic Ash Soils: Genesis, properties and utilization*. Elsevier Science Publishers B.V. Amsterdam, The Netherlands.

So, Ei-Kon. 1998 Statistical correlation between allophane content and index properties for volcanic cohesive soil. *Soils and Foundations* 38(4):85-93.

Tang, A-M. Cui, Y-J & Le, T-T. 2005. Thermal properties of compacted bentonites. *Canadian Geotechnical Journal* (submitted).

Tazaki, K. Tiba, T. Aratani, M. & Miyachi, M. 1992 Structural water in volcanic glass. *Clays and Clay Minerals* 40(1):122-127.

Terlien, M.T.J. 1997. Hydrological landslide triggering in ash-covered slopes of Manizales (Colombia). *Geomorphology* 20:165-175.

Townsend, F.C. 1985. Geotechnical characteristics of residual soils. *Journal of Geotechnical Engineering* 111(1):77-94.

Ugolini, F. & Dahlgren, R.A. 2004. Soil development in volcanic ash, *Global Environmental Research* Vol.6 No.2. Association of International Research Initiatives for Environmental Studies (AIRIES), Japan.

USDA. 1950. Diagnosis and improvement of saline and alcali soils. *USDA Agricultural Handbook No. 60*. United States Department of Agriculture.

Valencia, C.L. 1988. Geotectonica regional del Antiguo Caldas con énfasis en la aplicación de la ingeniería sísmica. Unpublished Msc. Thesis, Los Andes University, Bogotá, Colombia.

Wada, S. & Wada, K. 1977. Density and structure of allophane. *Clay Miner*. 12: 289-298.

Wada, Koji 1989. Allophane and imogolite. In: *Minerals in Soil Envieronment*, J.B. Dixon & S. B. Weed (Editors), SSSA Madison, WI, USA., p. 1051-1087.

Wada, K. 1990. Minerals and mineral formation in soils derived from volcanic ash in the tropics. *Prooceedings of the 9th International Clay Conference*, Strasbourg, 1989. V.C. Farmer & Y. Tardy (Eds). Sci. Géol. Mém., 85, p. 69-78, Strasbourg, 1990.

Wan, Yongshan. Kwong,, J. Brandes, H.G. & Jones, R.C. 2002. Influence of amorphous clay-size materials on soil plasticity and shrink-swell behavior. *Journal of Geotechnical and Geoenvironmental Engineering* 128(12).

Warkentin, B.P. & Maeda, T. 1974. Physical properties of allophane soils from the West Indies and Japan. *Soil Science Society of American Proceedings*. 38: 372.

Wells, N. & Northey, R.D. 1984. Shearing characteristics of an allophonic soil. *Clay Science* 6:93-101.

Wells, N. & Theng, B.K.G. 1988. The cracking behavior of allophone and ferrihydrite rich minerals: effect of pretreatment and material amendments. *Applied Clay Science* 3: 237-252.

Wesley, L.D. 1973. Some basic engineering properties of halloysite and allophane clays in Java, Indonesia. *Géotechnique* 23(4): 471-494.

Wesley, L.D. 1977. Shear strength properties of halloysite and allophane clays in Java, Indonesia *Géotechnique* 27(2): 125-136.

Wesley, L.D. 1996. Influence of structure and composition on residual soils. *Journal of Geotechnical Engineering* 166(4).

Wesley, L.D. 2001. Consolidation behavior of allophane clays. *Géotechnique* 51(10): 901-904.

Wesley, L.D. 2003. Geotechnical properties of two volcanic soils. *Geotechnics on the volcanic edge.* Tauranga, March 2003. New Zealand Geotechnical Society Symposium. The Institution of Professional Engineers New Zealand.

Wohletz, K & Krinsley, D. 1982. Scanning electron microscopy of basaltic hydromagmatic ash. *Los Alamos National Laboratory Report*, LA-UR 82-14 p. 33- 43.

Yun, T. S. & Santamarina, J. C. 2005. Decementation, softening and collapse: changes in small-strain shear stiffness in ko-loading. Journal of Geotechnical and Geoenvironmental Engineering, ASCE, 131(3):.350-358.

Table 1. Mineralogical composition (Location: Manizales. Depth: 7.0 m)

Fraction	Test	Mineral	z=1.5 m	z=5.5 m	z=7.0 m
Clay fraction (diameter < 2 µm)	X-ray Diffraction	Halloysite – 10Å	> 50%	~ 74%	~ 65%
		Mica	-	~ 9%	~ 12%
		Critobalite	15 – 30%	Traces	~ 20%
		Feldspars	Traces	-	-
		Minerals 2:1, 2:2	-	~ 14%	Traces
		Non quantifiable material by XRD	Present but non quantifiable	-	-
Coarse fraction (50 – 250 µm)	Analysis in polarizing microscope for petrology	Volcanic glass	18%	20%	22%
		Feldspar plagioclase	51%	45%	17%
		Hornblend	21%	24%	8%
		Hyperstone	4%	4%	-
		Magnetite	Traces	4%	49%
		Biotite	Traces	2%	3%
		Lamprobolite	Traces	Traces	Traces
		Tuff fragments	6%	-	-
		Lithic fragments	Traces	-	-

Note: See similar results in Arango, 1993.

Table 2 Volcanic ash soils in Colombia and around the world - Index properties

Properties	**Colombia**		**Other countries**		
pH	4.5 – 6.2 6.1 – 6.3 5.1 – 5.8	[2] [3] [4]	6 4.6 – 5.2 3.6 – 8 4.8 – 7.2 5.7 – 6.2 5.8 – 6.7	India USA Japan New Zealand Java Hawaii	[19] [5] [18] [14] [22] [23]
G_s	2.47 – 2.65 1.92 – 2.67 2.50 – 2.67	[4] [1] [28]	2.58 – 2.59 2.67 – 2.74 2.28 – 2.65	Ecuador Japan Fiji	[13] [11] [7]
S_a [m^{2}g^{-1}]	170 – 340	[28]	50 – 250 581 Allophane (N_2 adsorption)	Japan –	[18] [17]
e	2.0– 7.0 1.1 – 1.9 2.0 – 2.7 0.88 – 3.62 1.3 – 3.8	[3] [21] [4] [1] [28]	2.4 – 5.3, 1.5 – 8 1.9 – 4.1 allophane predominant 3.0 – 5.7, 1.0 – 6.1 1.8 – 6.6	Indonesia India Japan Java	[25, 27] [20] [6, 9] [22]
w_o	80 – 200% 16 – 90% 29 – 119%	[3] [1] [28]	50 – 300% 50 – 100% 102 – 205%, 40 – 50%, 27 – 184%	Indonesia India Japan	[27] [19] [6, 11, 9]
w_L	52 – 64% 60 – 70% 120 – 250 % 37 –117%	[4] [12] [15] [28]	70 – 110% halloysite predominant 85 – 190% allophane predominant 95 – 107% halloysite predominant 156 – 165% allophane predominant 179 – 187% 80 – 213% 72 – 159%, 31 – 40% 105 – 107%	Indonesia Indonesia New Guinea New Guinea Indonesia India Japan Ecuador	[25] [25] [10] [10] [26] [19] [18, 11] [8]
w_P	27 – 33% 45 – 50% 70 – 150% 25 – 90%	[4] [12] [15] [28]	55 – 75% halloysite predominant 65 – 150% allophane predominant 65 – 73% halloysite predominant 119 – 129% allophane predominant 139 – 149% 40 – 100%, 17 – 20% ~ 60%	Indonesia Indonesia New Guinea New Guinea Indonesia Japan Ecuador	[25] [25] [10] [10] [26] [18, 11] [8]
S_r	65 – 88%	[28]	50 – 80% > 95%	India Japan	[16] [6]
γ_{dry} [kN/m^3]	8.70 (sandy silt) 10.7 (silty sand) 7.0 – 8.4 4.5 – 13.8 5.7 – 13.8	[21] [21] [4] [1] [28]	4.0 – 7.2, 3.8 – 12.7 7.9 – 9.8 4.3 – 7.6	Japan Fiji Java	[6, 9] [7] [22]
γ_{sat} [kN/m^3]	15.1 (sandy silt) 16.1 (silty sand) 12.8 – 13.1	[21] [21] [28]	13.3 – 14.9 11 – 14 21.8 – 25.7	India Ecuador Japan	[19] [13] [9]
Fraction Sand	5 – 40%	[28]	0 – 30%* 25 – 59%**	* New Zealand ** West Indies and Japan	[20] [24]
Silt	55 – 70%		52 – 76%* 23 – 51%**		
Clay	5 – 25%		21 – 42%* 17 – 19%**		

References: [1] Arango, 1993, [2] Benavides, 1982, [3] Forero et al., 1999, [4] IGAC, 1996, [5] Johnson-Maynard et al., 1997, [6] Kitazono et al., 1987, [7] Knight, 1986, [8] Mendoza, 1985, [9] Miura, 2003, [10] Moore and Styles, 1988, [11] Moroto, 1991, [12] Olarte, [13] O'Rourke and Crespo, 1988, [14] Parfitt and Kimble, 1989, [15] Rivera J.D., 2003, [16] Rouse et al 1986, [17] Shoji, 1993, [18] So, 1998, [19] Rao, 1995, [20] Rao, 1996, [21] Terlien, 1997, [22] Van Ranst et al., 2002, [23] Wada, 1990, [24] Warkentin and Maeda, 1974, [25] Wesley, 1977, [26] Wesley, 2001, [27] Wesley, 2003, [28] This study.

Table 3 Drying-induced changes in Atterberg limits

Properties	**Condition**	**Colombia**		**Ecuador** [2]	**New Guinea** [3]
w_L	Natural	117% 81 – 94% 112 – 183% 104 – 200% 97 – 111%	[5] [4] [1] [1] [1]	105 – 107%	Halloysite predominant: 95 – 107% Allophane predominant: 156 – 165%
	Oven dried	59% 74 – 76% 57 – 94% 51 – 66% 64 – 70%	[5] [4] [1] [1] [1]	59%	Halloysite predominant: 61 – 65% Allophane predominant: 44%
w_P	Natural	90% 45 – 50% 82 – 113% 57 – 98% 73 – 76%	[5] [4] [1] [1] [1] [1]	~ 60%	Halloysite predominant: 65 – 73% Allophane predominant: 119 – 129%
	Oven dried	46% 42 – 45% 46 – 80% 49 – 64% 56 – 58%	[5] [4] [1] [1] [1]	46%	Halloysite predominant: 46 – 47% Allophane predominant: 42%

References: [1] Arango, 1993, [2] Mendoza, 1985, [3] Moore and Styles, 1988, [4] Rivera, 2003, [5] This study

Table 4 Engineering properties of volcanic ash soils (Colombia and worldwide)

Properties	**Colombia**		**Other countries**		
k [m/s]	8.1×10^{-7} – 16×10^{-5} 8.1×10^{-7} (sandy silt) 4.4×10^{-6} (silty sand) 7.0×10^{-8}	[3] [10] [10] [6]	2.0×10^{-5} 3.0×10^{-5} 1.0×10^{-9} – 1.3×10^{-8} halloysite predominant 0.8×10^{-9} – 2.7×10^{-8} allophane predominant 1.4×10^{-6} – 5.6×10^{-6}	Ecuador Costa Rica Indonesia Indonesia Dominica	[4] [4] [11] [11] [8]
ϕ [°]	26 – 43 29 – 39 (silty sand) 22 – 29 (sandy silt) 30 – 38	[5] [10] [10] [6]	30 – 40 29 – 41	Indonesia Dominica	[12] [7]
q_u [Kpa]	26 – 309 25 – 135	[1] [6]	65 – 200 100 – 230 20 – 160	Indonesia - NZ Japan Japan	[12] [4] [5]
V_s [m/s]	100 – 210 100 – 180	[2] [13]	135 – 175	Japan	[9]

References: [1] Arango, 1993, [2] Forero et al., 1999, [3] Imeson and Vis, 1982, [4] Maeda et al., 1977, [5] Moroto, 1991, [6] Olarte, [7] Rao, 1995, [8] Rao, 1996, [9] Sahaphol and Miura, 2005,[10] Terlien, 1997, [11] Wesley, 1977, [12] Wesley, 2003, [13] This study.

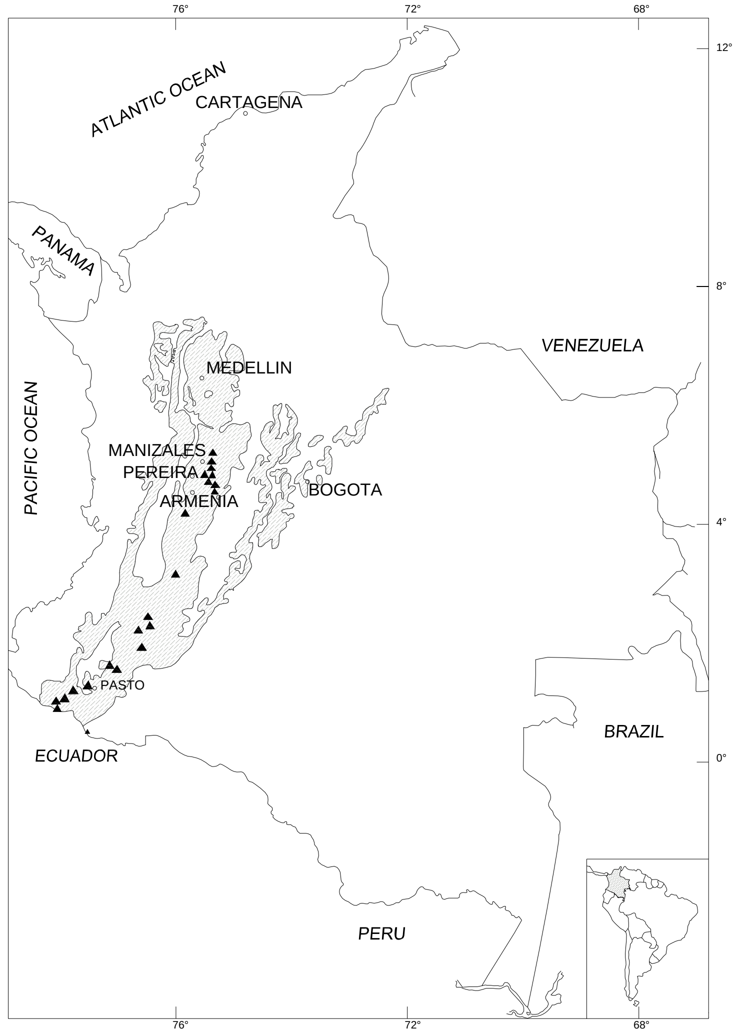

Figure 1 Spatial distribution of volcanoes (▲) and volcanic ash soils (shaded area) in Colombia (modified from IGAC, 1995). About 12% of the national territory is covered with volcanic ash soils.

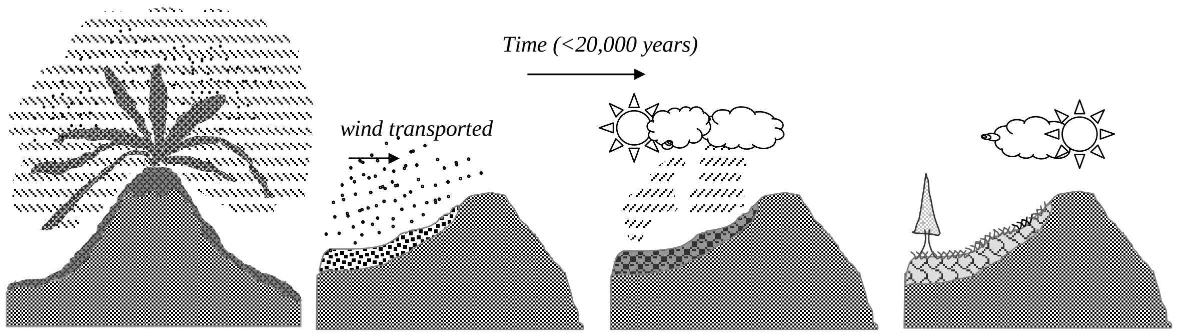

Eruption	***"Volcanic Ash"***	***Diagenesis***	***"Volcanic Ash Soil"***
Cloud of pyroclasts (volcanic ashes, lapilli, bombs)	$e \sim 0.8-1.7$ $\mu m < d_{particle} < cm$ Composition: sillicates and volcanic glass Other minerals: felspars, quartz, hornblend, hypersthene, augite, magnetite	Dissolution of parent minerals Leaching of silica Iron and aluminium content increases Reprecipitation into new minerals	$e = 2.0 – 7.0$ $S_s = 170 – 340\ m^2 g^{-1}$ High water retention potential New clay minerals: halloysite, allophane and imogolite Cemented structure

Figure 2 The formation of volcanic ash soils

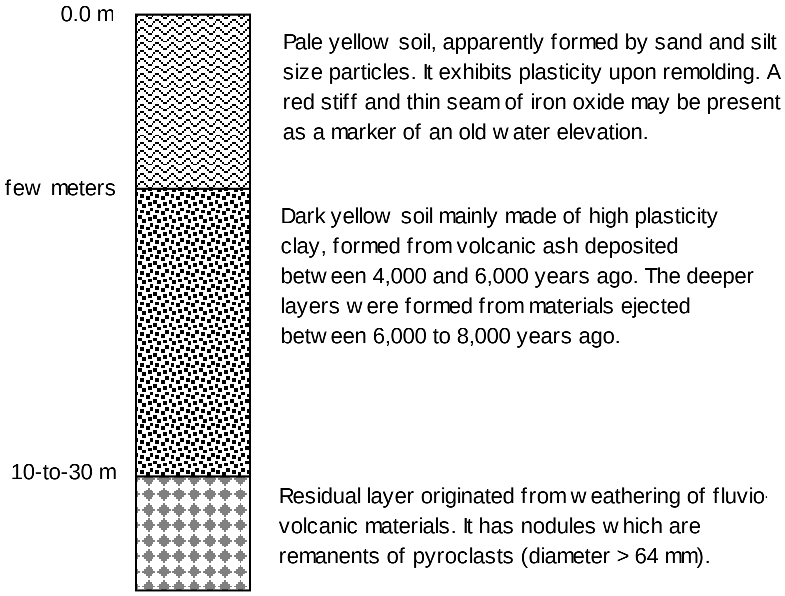

Pale yellow soil, apparently formed by sand and silt size particles. It exhibits plasticity upon remolding. A red stiff and thin seam of iron oxide may be present as a marker of an old water elevation.

Dark yellow soil mainly made of high plasticity clay, formed from volcanic ash deposited between 4,000 and 6,000 years ago. The deeper layers were formed from materials ejected between 6,000 to 8,000 years ago.

Residual layer originated from weathering of fluvio-volcanic materials. It has nodules which are remanents of pyroclasts (diameter > 64 mm).

Figure 3 Typical profile of volcanic ash soils in Colombia. General rule: deeper and older → finer and more clayey

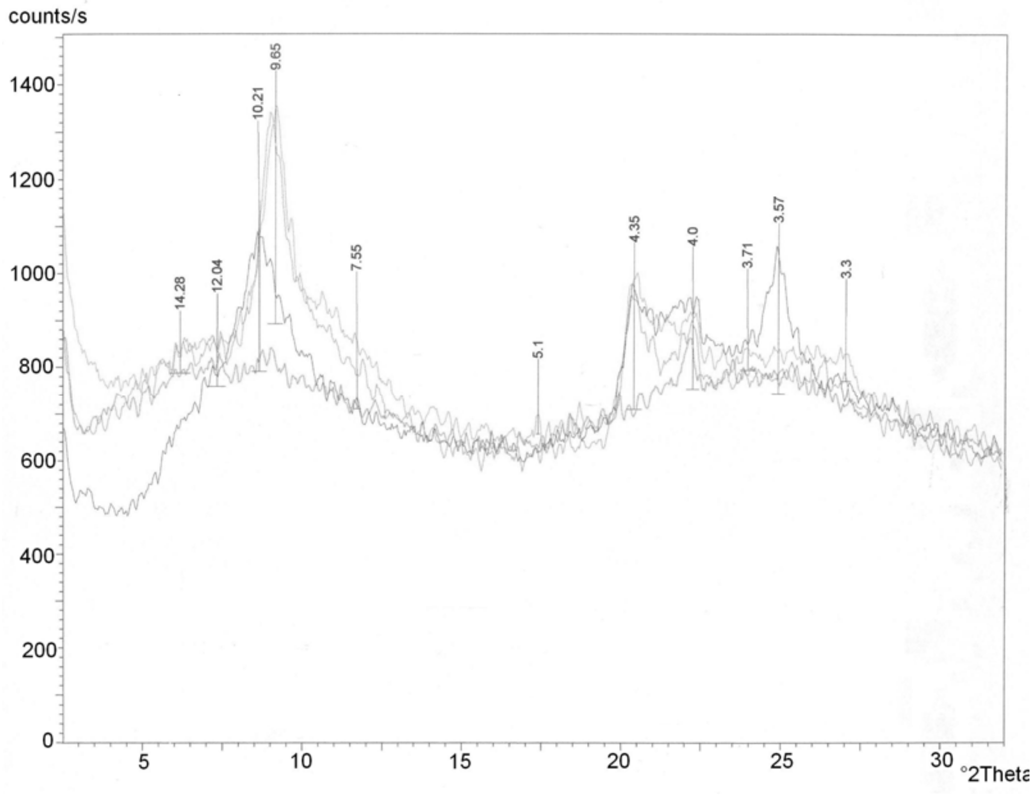

Figure 4 X-ray diffraction patterns for different specimen preparation methods (Location: Manizales. Depth: 7.0 m)

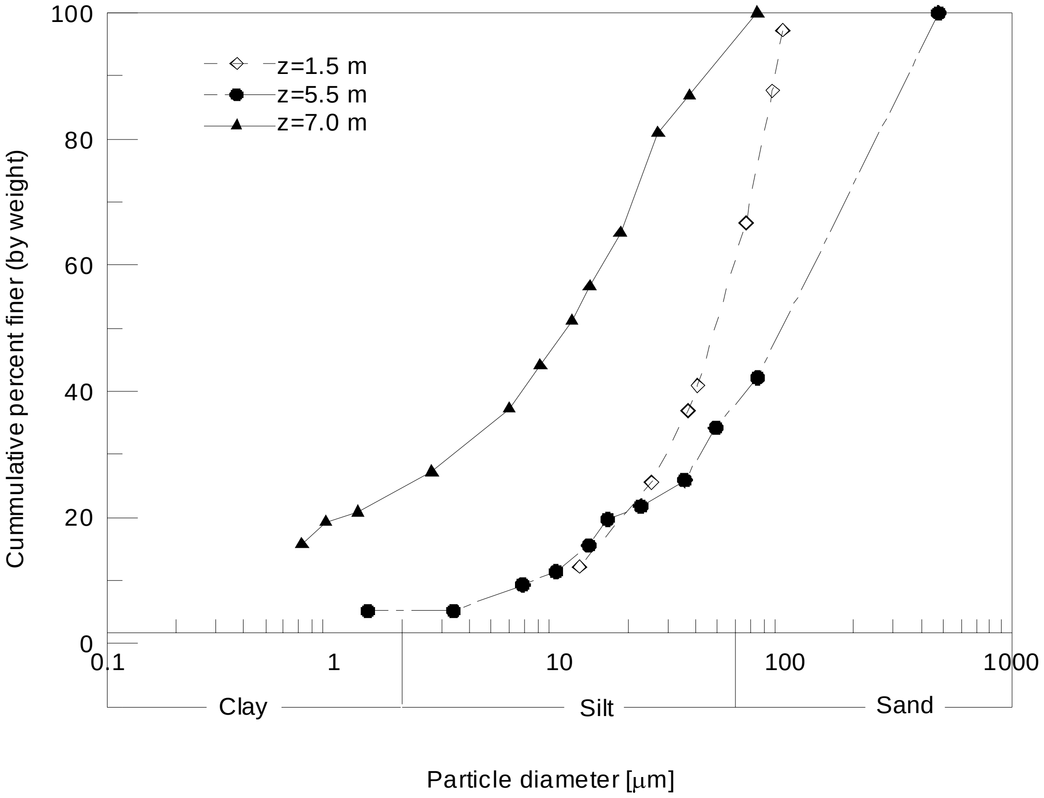

Figure 5 Particle size distribution (Location: Manizales – Different depths)

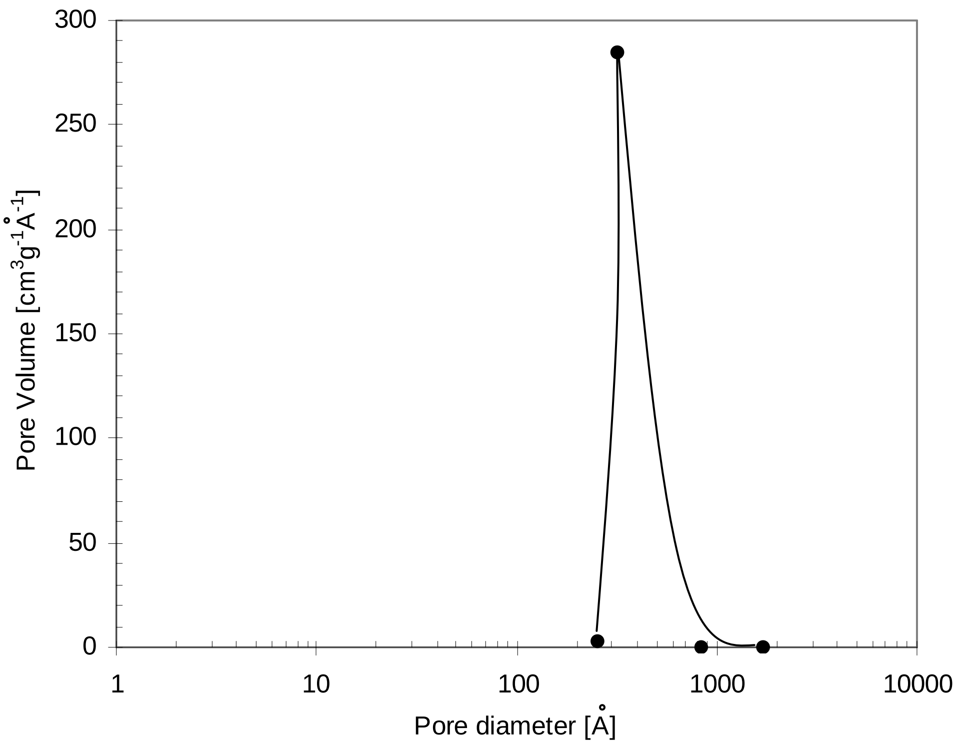

Figure 6 Pore size distribution of Colombian volcanic ash soils (Location: Manizales. Depth: 7.0 m)

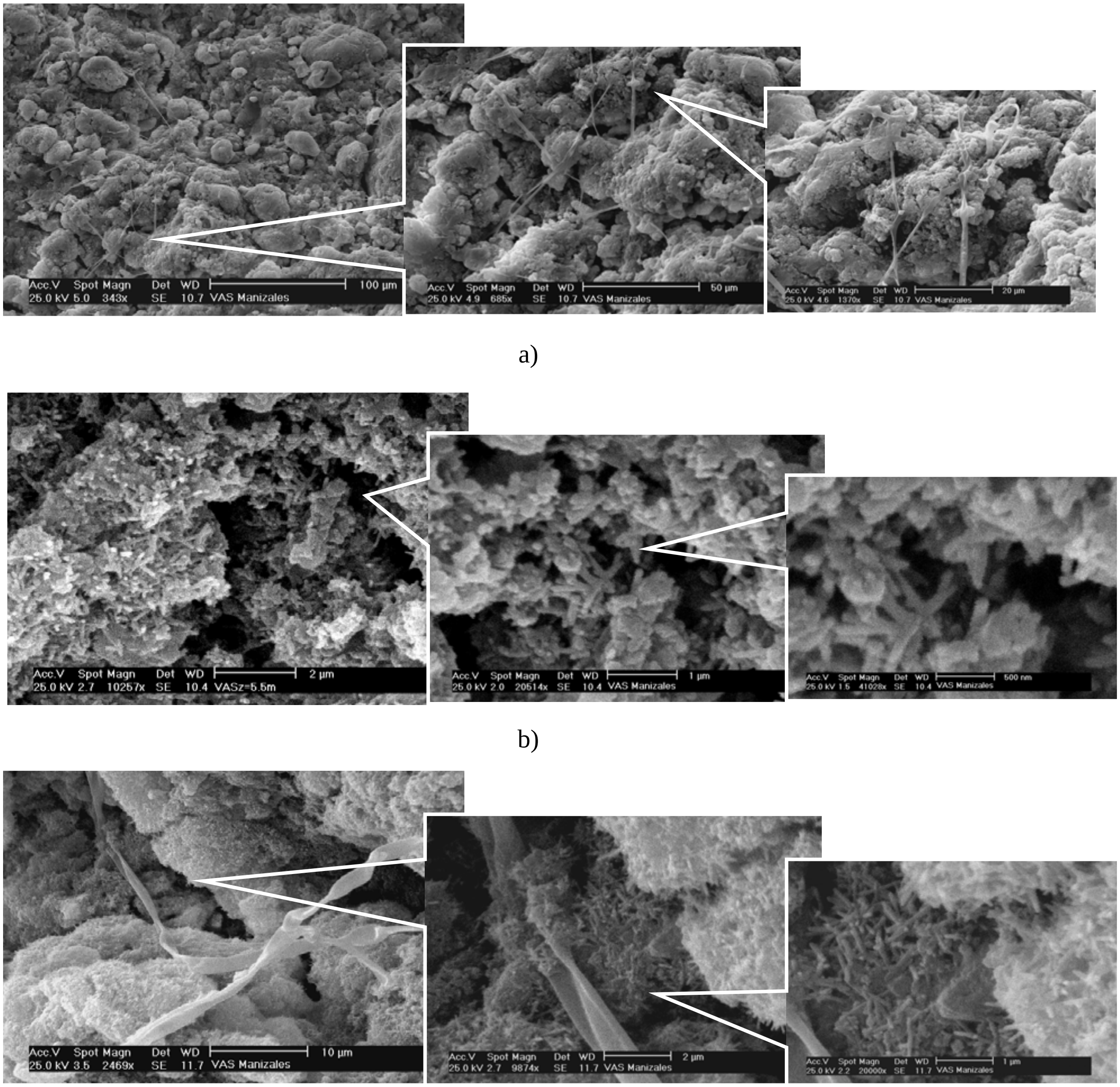

a)

b)

c)

Figure 7 SEM images obtained at different magnification (Location: Manizales. Depth: 7.0 m)

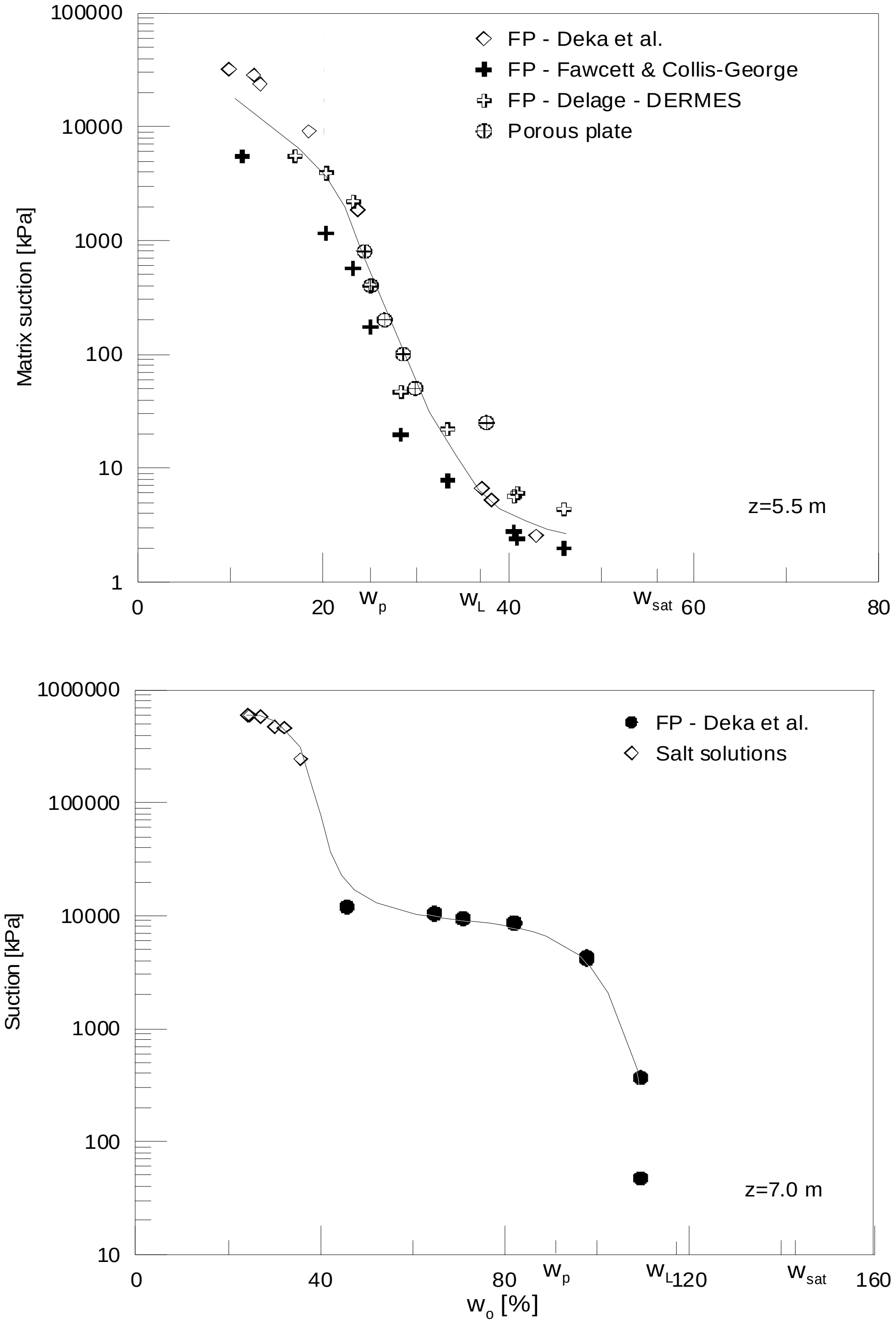

Figure 8 Characteristic water retention curves for Colombian volcanic ash soils (Location: Manizales. Depth: z=5.5 m and z=7 m). Results using filter paper technique FP are interpreted following the different listed authors.

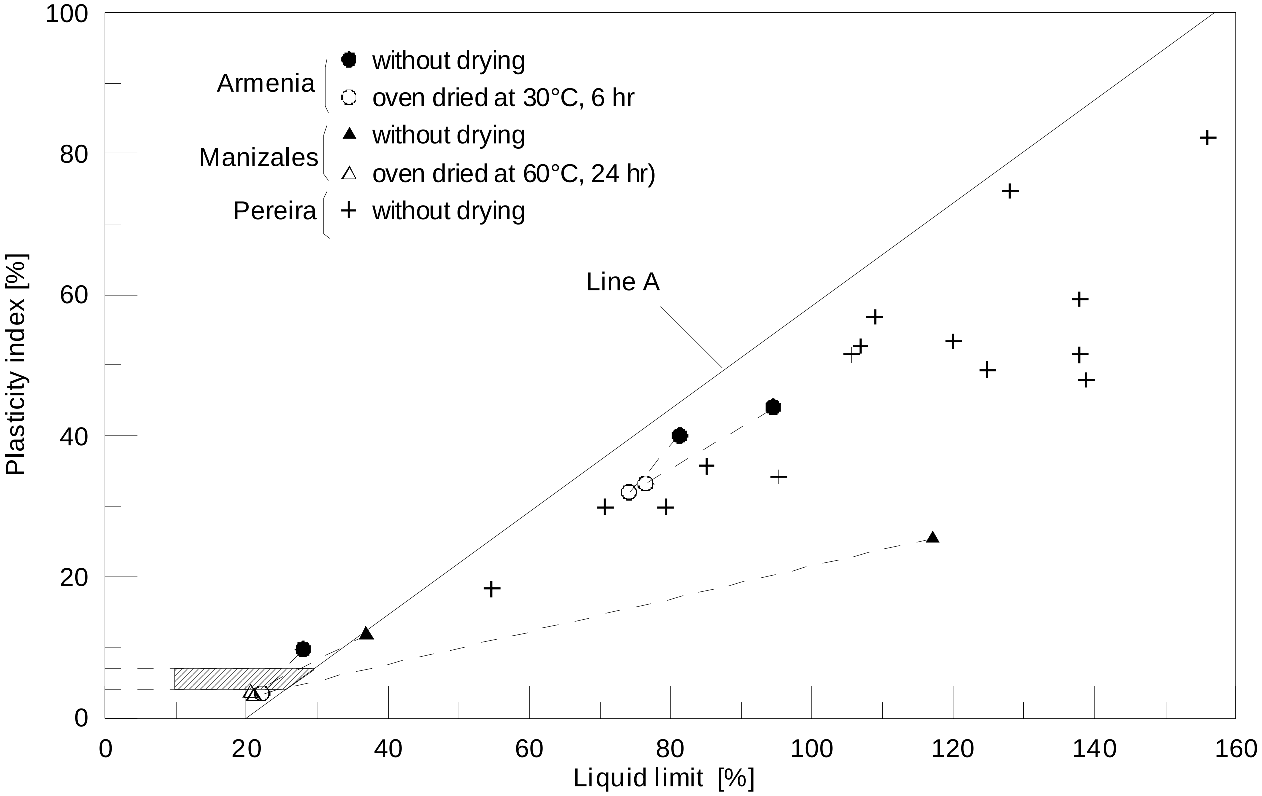

Figure 9 Plasticity of Colombian volcanic ash soils (Data for Pereira gathered by Uniandes, 2001)

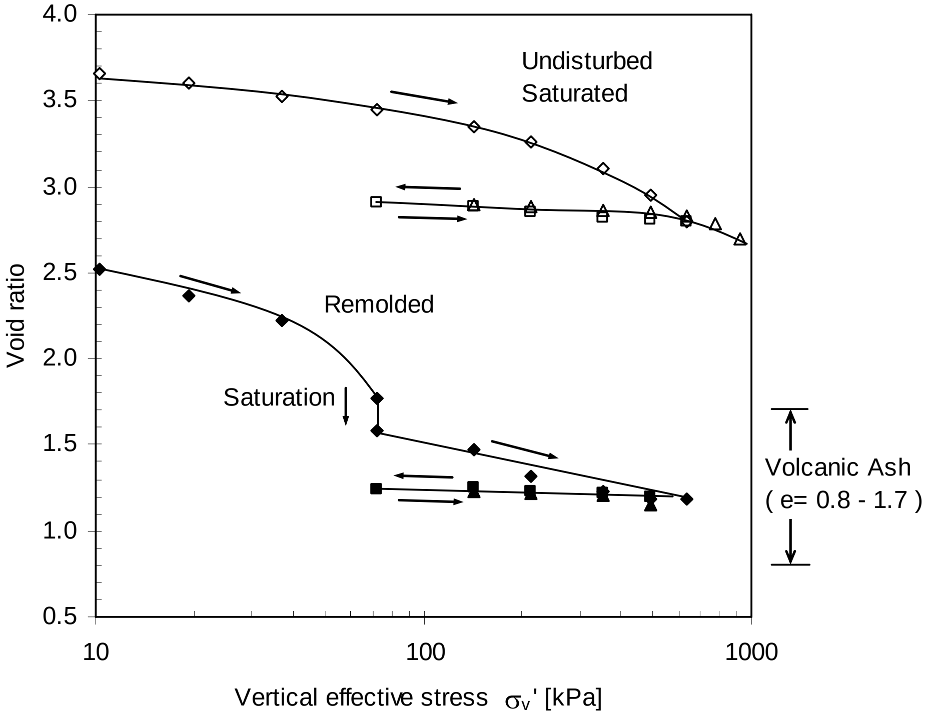

Figure 10 Void ratio vs. effective stress – Undisturbed specimen saturated at zero confinement and remolded specimen prepared with ground material passing sieve No. 200 and saturated at σ_v'=72 kPa.

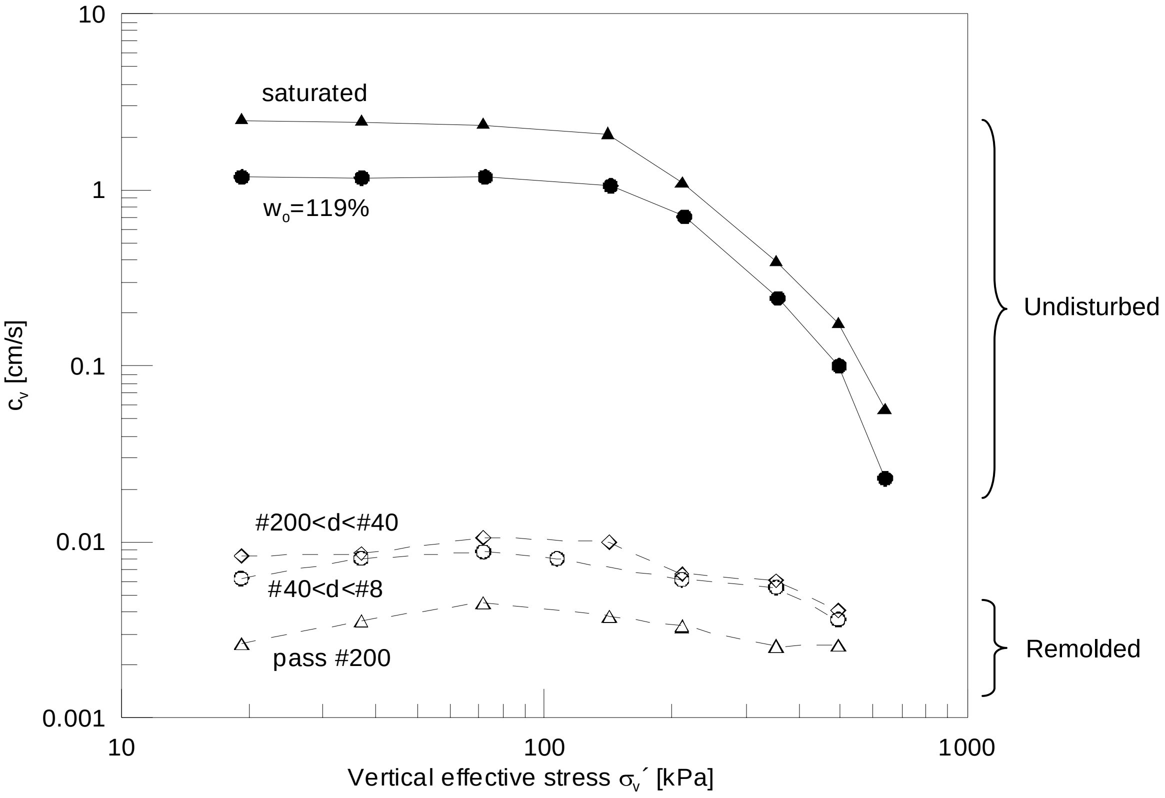

Figure 11 Coefficient of consolidation vs. confining stress – Data gathered during k_o loading. (Location: Manizales. Depth: 7.0 m)

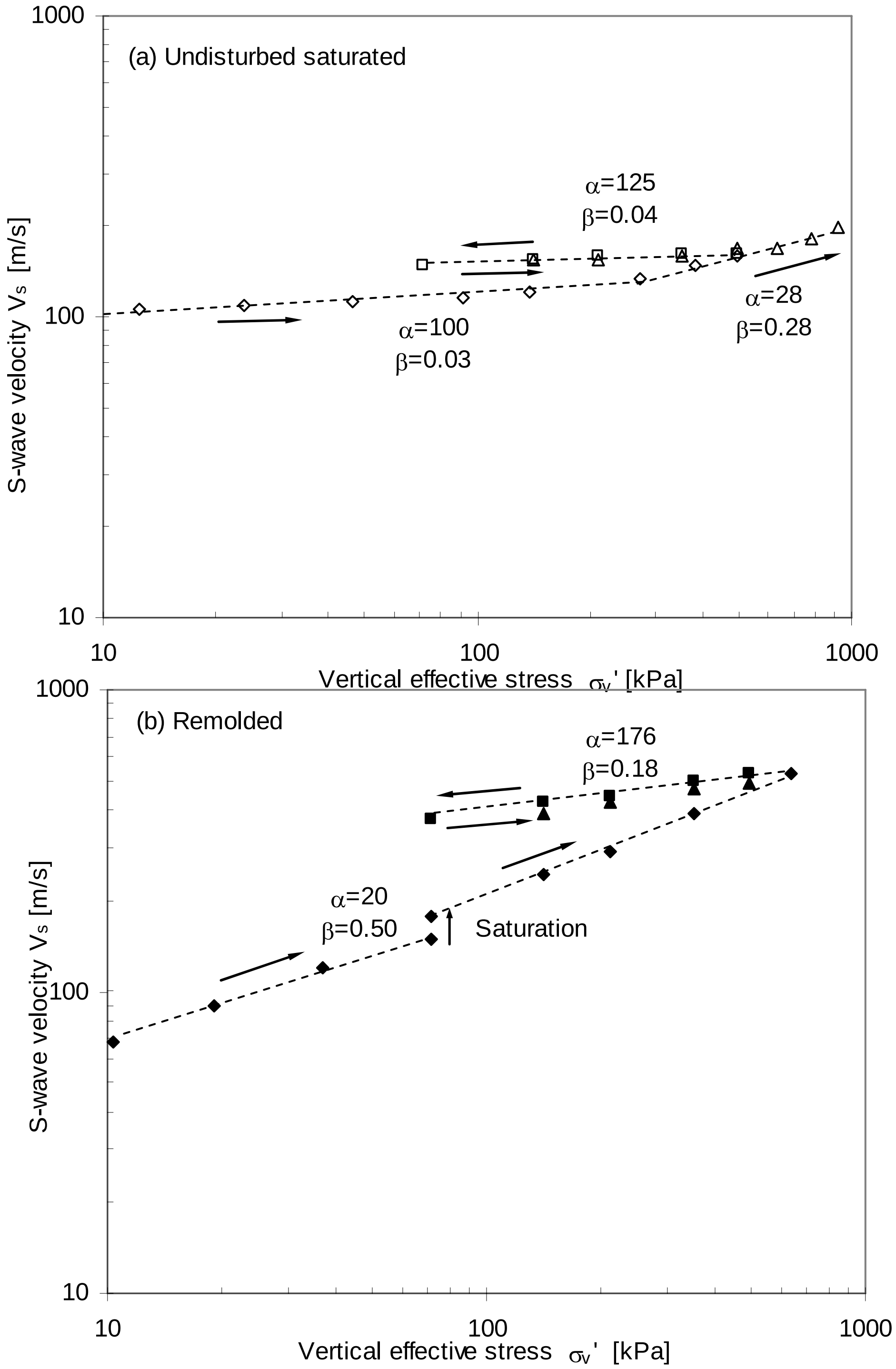

Figure 12 Shear wave velocity vs. effective stress. a) Undisturbed specimen saturated at zero confinement. b) Remolded specimen prepared with ground material passing sieve No. 200 and saturated at σ´v=72 kPa (specimen from: Manizales. Depth: 7.0 m)

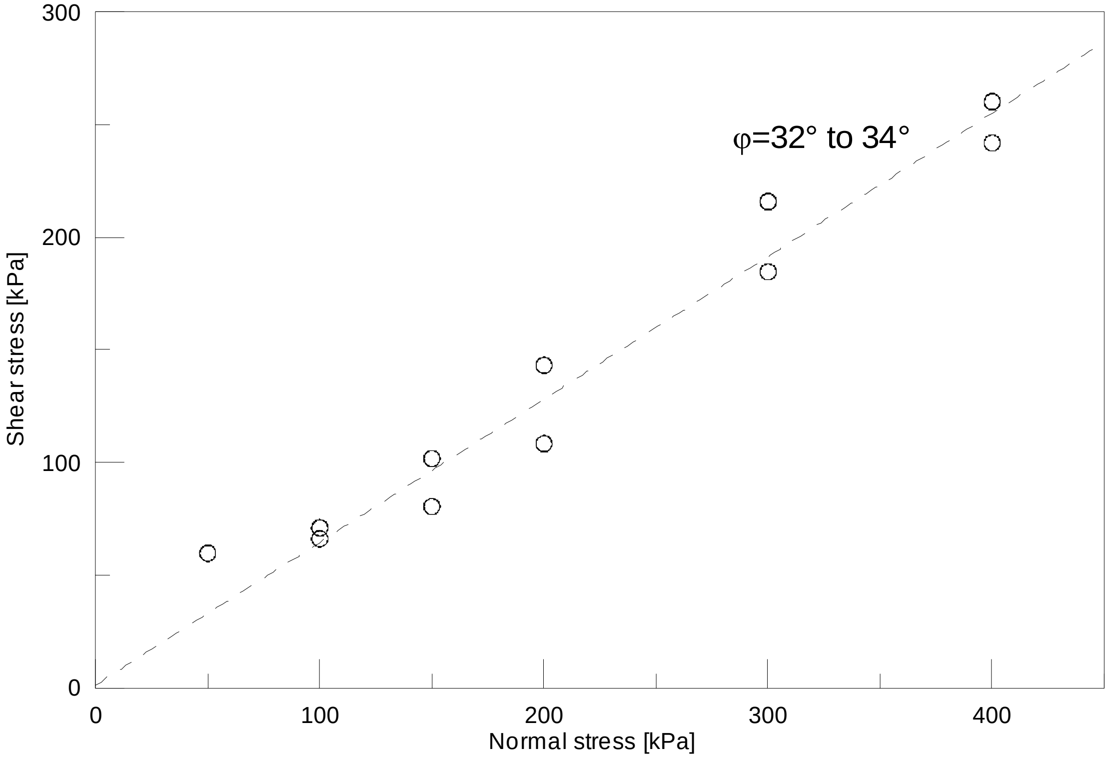

Figure 13 Drained direct shear test data – Saturated specimens (Location: Manizales. Depth: 5.5 m)

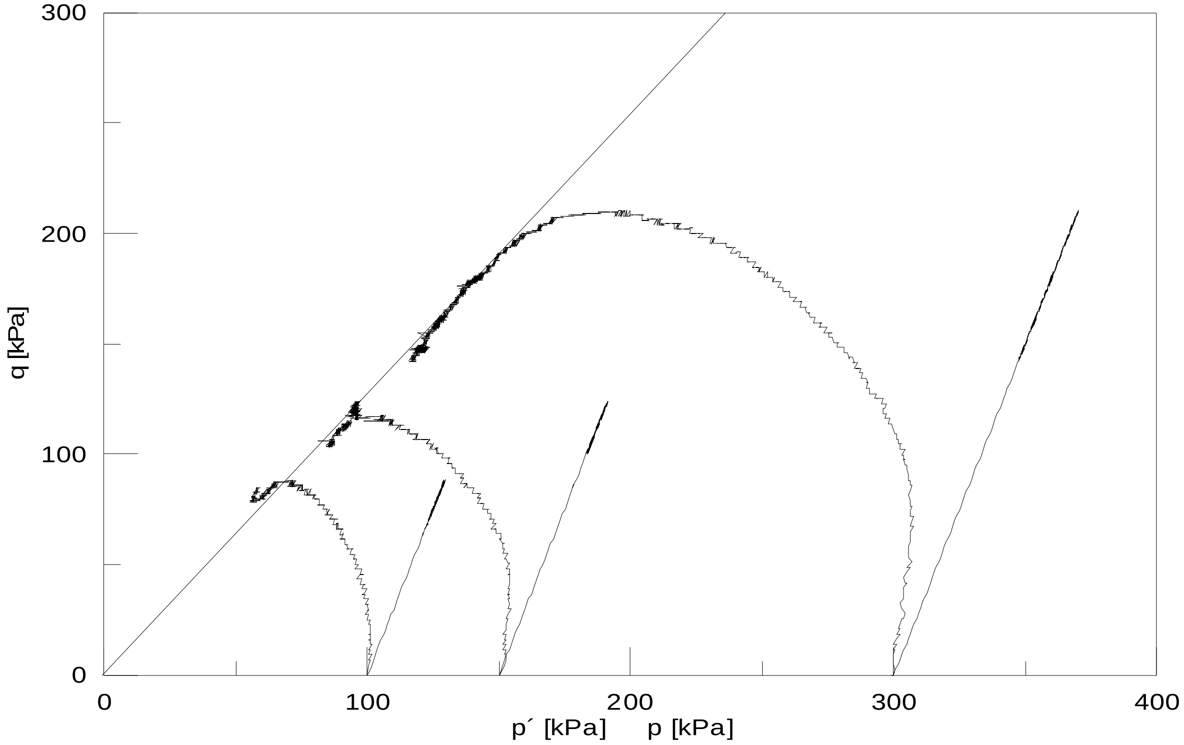

Figure 14 CU triaxial test data – Saturated specimens (Location: Manizales. Depth: 7.0 m)

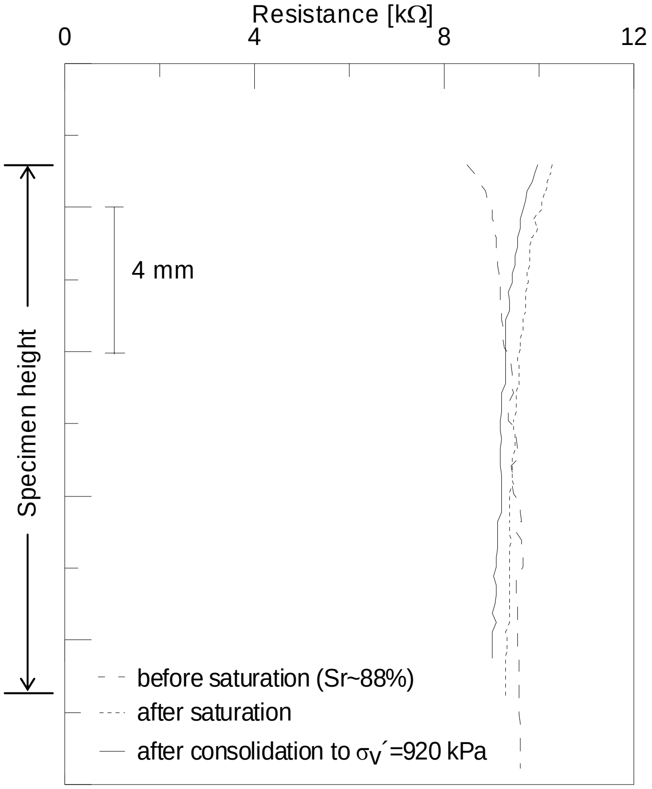

Figure 15 Electrical resistance profile - Undisturbed specimen under different loading and moisture conditions. (Location: Manizales. Depth:: 7.0 m)

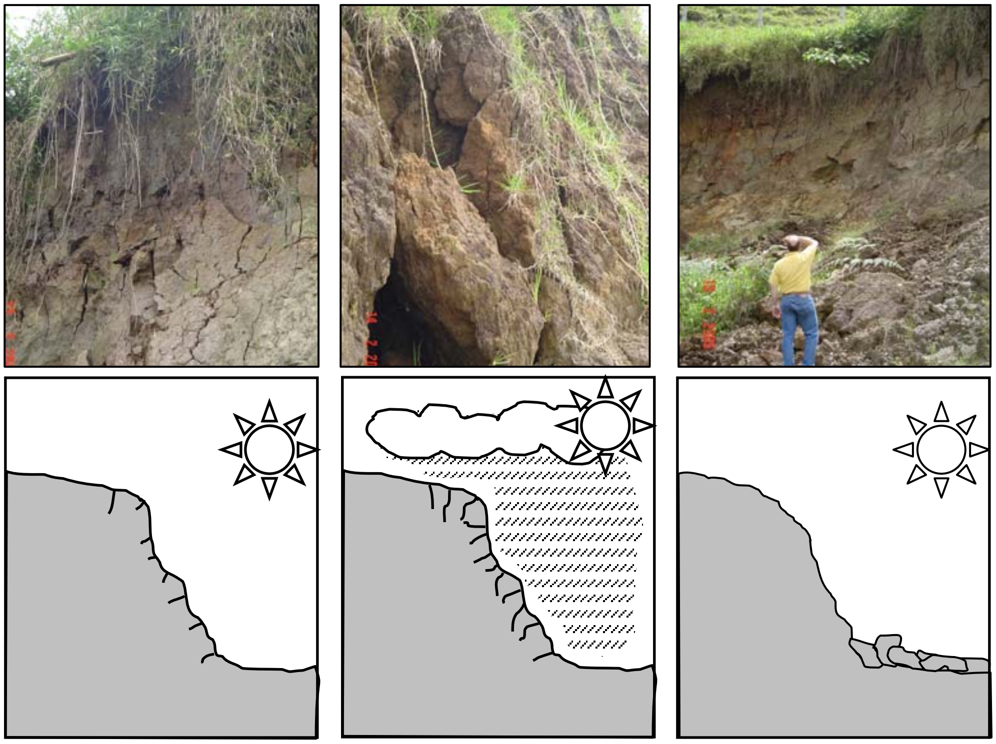

Figure 16 Gradual degradation of slopes (Pictures taken at Pereira – Armenia road)

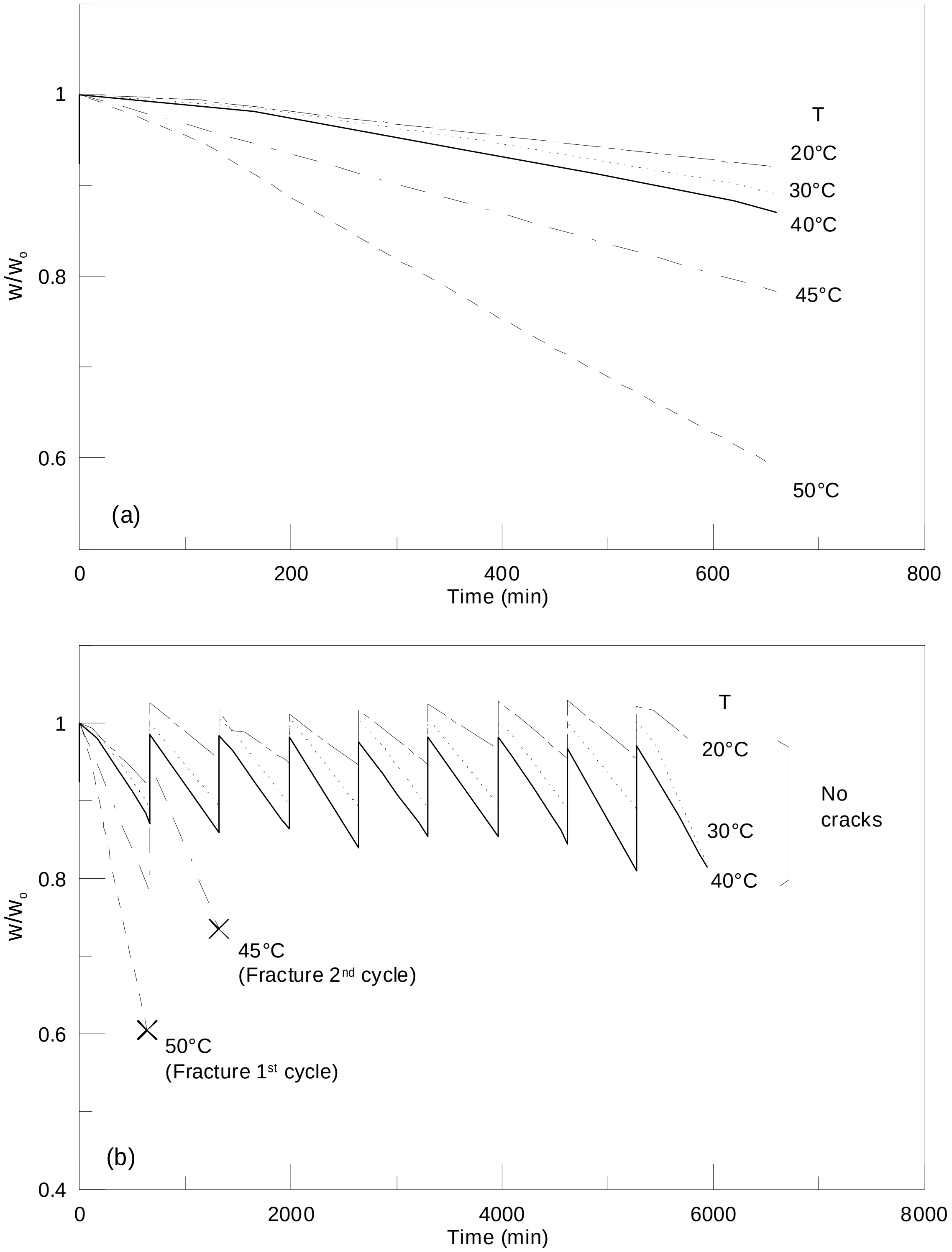

Figure 17 Drying and wetting cycles – Damage. (Location: Manizales. Depth: 7.0 m). (a) Moisture lost in once cycle. (b) Multiple cycles and crack formation

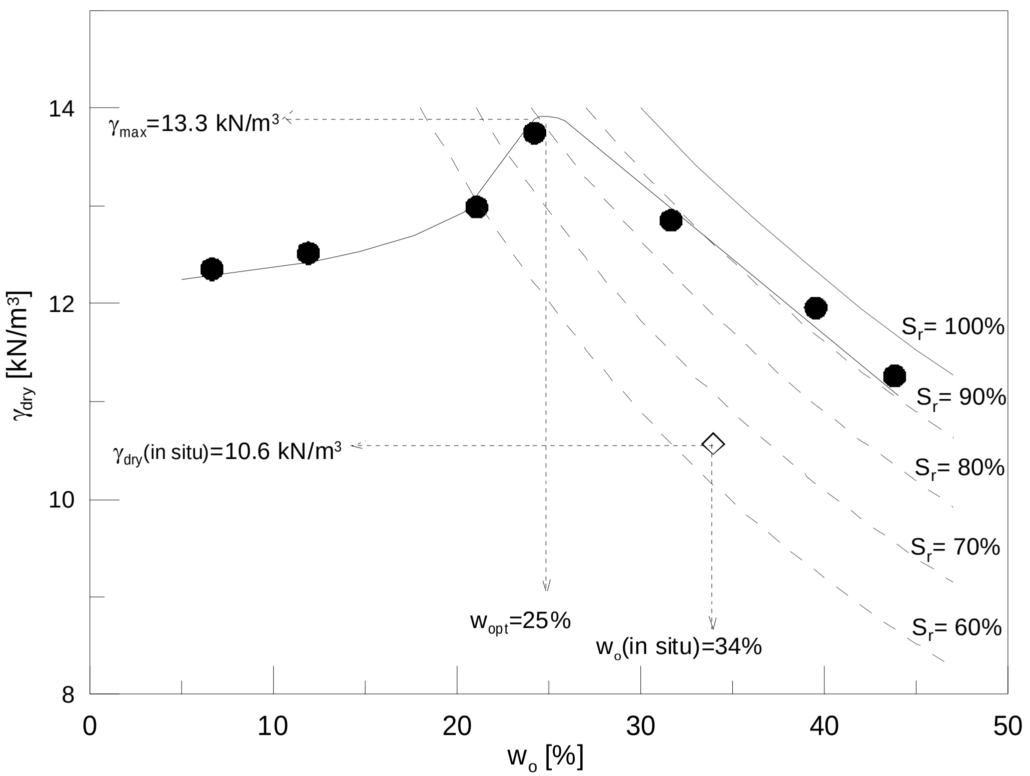

Figure 18 Compaction curve obtained with air dried soil, passing sieve No. 40 (Location: Manizales. Depth: 5.5 m)

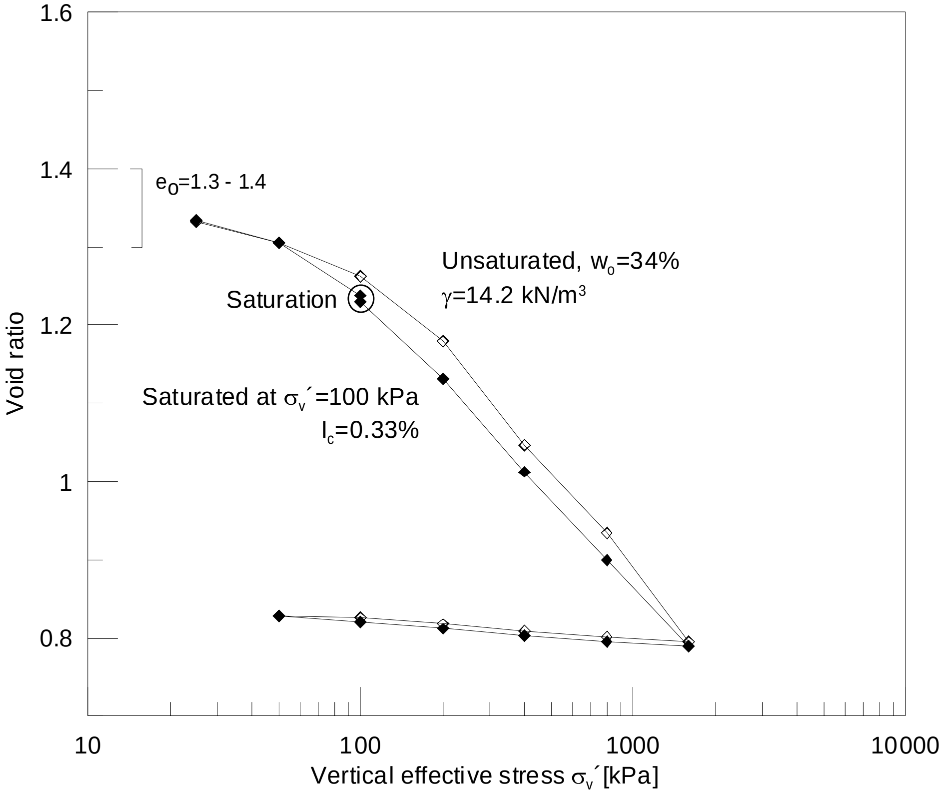

Figure 19 Oedometric test for remolded specimens prepared with grains passing sieve #40. One specimen is loaded at the in situ water content w_o=31%. The other is loaded to σ_v´=100 kPa and saturated before further loading. (Location: Manizales. Depth: 5.5 m)

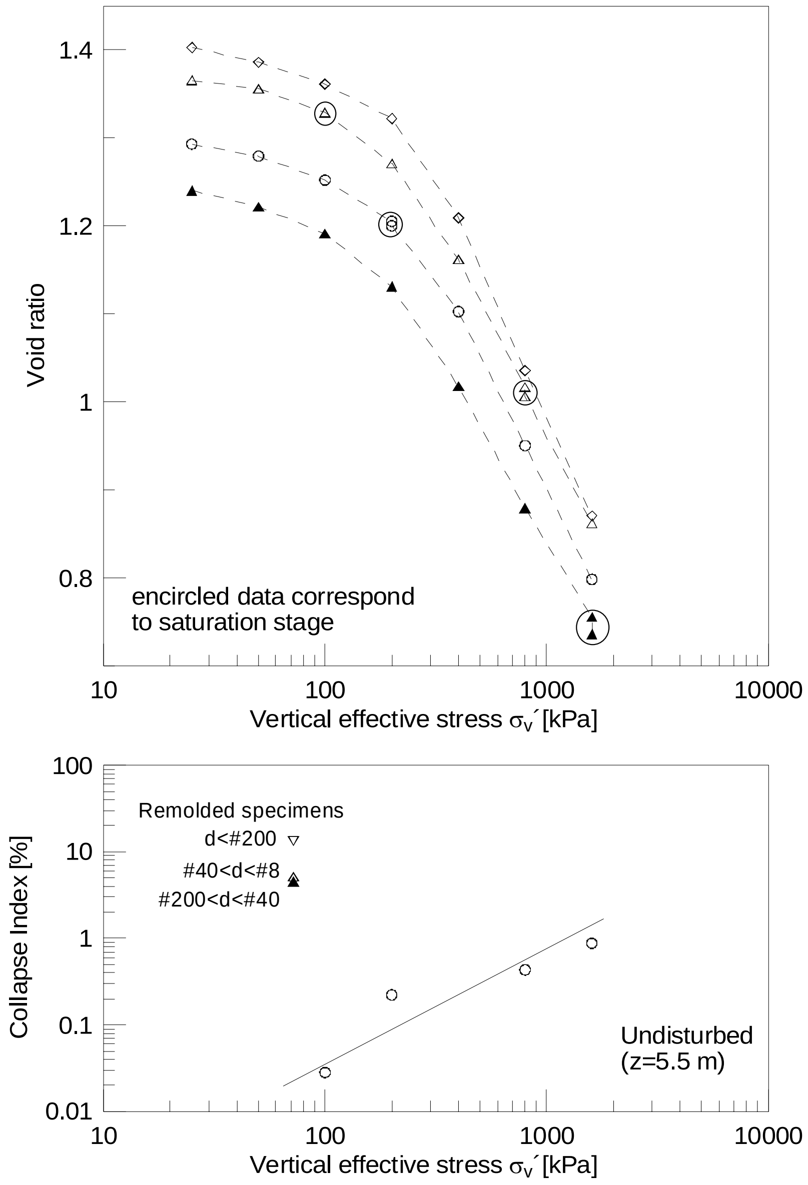

Figure 20 Collapse potential – Undisturbed specimens (Location: Manizales). For comparison values of collapse index I_c are shown for remolded specimens formed with different size fractions.